Global Crop Yield Reductions due to Surface Ozone Exposure: 2. Year 2030 Potential Crop Production Losses, Economic Damage, and Implications for World Hunger under Two Scenarios of O_3 Pollution

Shiri Avnery [a], Denise L. Mauzerall [b,*], Junfeng Liu [c], and Larry W. Horowitz [d]

[a] Program in Science, Technology, and Environmental Policy, Woodrow Wilson School of Public and International Affairs, 414 Robertson Hall, Princeton University, Princeton, NJ 08544, USA, savnery@princeton.edu

[b] Woodrow Wilson School of Public and International Affairs and Department of Civil and Environmental Engineering, 445 Robertson Hall, Princeton University, Princeton, NJ 08544, USA, mauzeral@princeton.edu

[c] NOAA Geophysical Fluid Dynamics Laboratory, 201 Forrestal Road, Princeton University, Princeton, NJ 08540, Junfeng.Liu@noaa.gov

[d] NOAA Geophysical Fluid Dynamics Laboratory, 201 Forrestal Road, Princeton University, Princeton, NJ 08540, Larry.Horowitz@noaa.gov

[*] Corresponding author.

Email: mauzeral@princeton.edu

Phone: +1 609-258-2498.

Fax: +1 609-258-6082

Submitted to *Atmospheric Environment* September 1, 2010.

Global Crop Yield Reductions due to Surface Ozone Exposure: 2. Year 2030 Potential Crop Production Losses, Economic Damage, and Implications for World Hunger under Two Scenarios of O_3 Pollution

Abstract

Here we examine the potential risk globally to three key staple crops (soybean, maize, and wheat) of surface ozone (O_3) exposure in the near future (year 2030). We use two different trajectories of O_3 precursor emissions—the Intergovernmental Panel on Climate Change Special Report on Emissions Scenarios A2 and B1 storylines, which represent upper- and lower-boundary projections, respectively, of most O_3 precursor emissions. We use simulated hourly O_3 concentrations from the Model for Ozone and Related Chemical Tracers version 2.4 (MOZART-2), satellite-derived datasets of agricultural production, and field-based concentration:response relationships to calculate crop yield reductions, their associated costs (the economic value of crop production losses), and the number of people who could potentially avoid undernourishment if crop reductions due to O_3 exposure were eliminated. We compare our results to those of our companion paper, in which we examined the impact of O_3 on agricultural yields in the year 2000. Our results indicate that for the A2 scenario, global year 2030 relative yield loss of wheat ranges from 5.4-26% (a decrease in yield of 1.5-10% from year 2000 values), 15-19% for soybean (decrease of 0.9-11%), and 4.4-8.7% for maize (decrease of 2.1-3.2%) depending on the metric used, with total global agricultural losses worth \$17-35 billion USD_{2000} annually (+\$6-17 billion). We further estimate that the caloric equivalent of crop production losses under this scenario (119-231 million metric tons (Mt)) could lift 379-890 million individuals above minimum dietary energy requirements defined by the United Nations Food and Agriculture Organization (FAO)—2-3 times our year 2000 estimate. Under the B1 scenario, we project more modest but substantial reductions in yields: 4.0-17% for wheat (a decrease in yield of 0.1-1.8% from 2000), 9.5-15% for soybean (decrease of 0.7-1.0%), and 2.5-6.0% for maize (decrease of 0.3-0.5%), with total losses worth \$12-21 billion annually (+\$1-3 billion). We calculate that crop production loss under the B1 scenario (87-137 Mt) could potentially feed 283-545 million

people above the FAO-defined threshold for undernourishment. Because our analysis uses crop data from the year 2000, which likely underestimates agricultural production in 2030 due to the need to feed a rapidly rising global population, our calculations of crop production loss, economic loss, and potential avoided undernourished individuals are conservative. Our results suggest that O_3 pollution poses a growing threat to global food security even under the most optimistic scenario of future ozone precursor emissions, and that O_3 mitigation may be a valuable means to adequately feed a growing population without further environmental degradation.

Keywords: ozone; ozone impacts; agriculture; crop loss; integrated assessment; food security

1. Introduction

Surface ozone (O_3) is the most damaging air pollutant to crops and ecosystems (Heagle, 1989), produced in the troposphere by catalytic reactions among nitrogen oxides ($NO_x = NO + NO_2$), carbon monoxide (CO), methane (CH_4), and non-methane volatile organic compounds (NMVOCs) when sunlight is present. Ozone enters leaves through plant stomata during normal gas exchange. As a strong oxidant, ozone and its secondary byproducts damage vegetation by reducing photosynthesis and other important physiological functions, which may result in weaker, stunted plants, inferior crop quality, and decreased yields (Fiscus et al., 2005; Morgan et al., 2006; Booker et al., 2009; Fuhrer, 2009).

O_3 precursors are emitted by vehicles, power plants, biomass burning, and other sources of combustion. Over the past century, annual mean surface concentrations of ozone at mid- to high latitudes have more than doubled (Hough and Derwent 1990; Marenco et al., 1994). Although O_3 mitigation efforts have reduced peak ozone levels in both rural and urban areas of North America, Europe, and Japan in recent years, background levels continue to increase (Oltmans et al., 2006). In addition, ozone concentrations are expected to rise in developing countries due to increased emissions of nitrogen oxides and other ozone precursors associated with rapid economic expansion and industrialization (Nakićenović et al., 2000; Dentener et al., 2005; Riahi et al., 2007). Due to transport of O_3 pollution across national boundaries and continents (Fiore et al., 2009), rising O_3 precursor emissions in these nations are projected to increase hemispheric scale background O_3 concentrations and hence may pose a threat to both local and global food security.

The demonstrated phytotoxicity of O_3 and its prevalence over important agricultural regions around the world demand an assessment of the magnitude and distribution of ozone risk to global food production under present-day and future O_3 concentrations. In the first of our two-part analysis (Avnery et al., 2010), we calculated global yield losses of three key staple crops (soybean, maize, and wheat) and their associated costs in the year 2000 using simulated O_3 concentrations by the Model for Ozone and Related Chemical Tracers version 2.4 (MOZART-2), observation-based crop production datasets, and concentration:response (CR) relationships derived from field studies. We estimated the value of crop production losses not only in terms of pecuniary damages, but also their caloric equivalent—which we used to calculate the potential number of undernourished individuals who might have been fed at minimum dietary energy requirements if not for O_3-induced reductions in crop yields. Our results indicated that year 2000 global yield reductions ranged from 8.5-14% for soybean, 3.9-15% for wheat, and 2.2-5.5% for maize depending on the metric used, with global crop production losses (79-121 million metric tons (Mt)) worth \$11-18 billion annually (USD_{2000}). These findings agree well with the only other estimate of global O_3-induced crop reductions and their economic value available in the literature (Van Dingenen et al., 2009), providing further evidence that the yields of major crops across the globe are already being significantly inhibited by exposure to surface ozone. We further estimated that the dietary energy equivalent of O_3-induced crop losses in 2000 could have lifted 21-36% of the year 2000 global undernourished population (180-312 million people) above the undernourishment threshold defined by the United Nations Food and Agriculture Organization (FAO).

Van Dingenen et al. (2009) (hereafter VD2009) additionally provide the first, and until now only, estimate of global crop yield losses due to ozone exposure in the near future (year 2030). VD2009 calculate crop losses as projected under the optimistic "current legislation (CLE) scenario", which assumes that presently approved air quality legislation will be fully implemented by 2030, and find that global crop yield reductions increase only marginally from the year 2000 (+2-6% for wheat, +1-2% for rice, and +<1% for maize and soybeans), with the most significant additional losses primarily occurring in developing nations. Unfortunately, the CLE scenario may be an overly optimistic projection of O_3 precursor emissions in many parts of the world, as enforcement often lags promulgation of air pollution regulations (Dentener et al., 2006). VD2009 may have therefore significantly underestimated the future risk to crops from surface ozone.

Here we calculate crop yield reductions due to O_3 exposure according to two different O_3 precursor emission scenarios: the Intergovernmental Panel on Climate Change (IPCC) Special Report on Emissions Scenarios (SRES) A2 and B1 storylines (Nakićenović et al., 2000), representing upper- and lower boundary trajectories, respectively, of ozone precursor emissions. We additionally estimate the associated costs of crop yield losses in terms of their monetary value and their contribution to global undernourishment as in Avnery et al. (2010). Through comparison with our year 2000 results, we identify agricultural winners and losers under each future scenario and nations where O_3 mitigation may be a particularly effective strategy to combat domestic hunger without the environmental damage associated with traditional methods of increasing crop production.

2. Methodology

2.1 Data sources

We use global crop production maps, simulated surface ozone concentrations from which we calculate O_3 exposure over crop growing seasons, and CR functions that relate a given level of ozone exposure to a predicted yield reduction to calculate global crop losses. Our first paper provides an in-depth description of our data sources and methods, which we briefly summarize and augment here (see Avnery et al., 2010 for further detail).

The global crop distribution datasets were compiled by Monfreda et al. (2008) and Ramankutty et al. (2008) using a data fusion technique, where two satellite-derived products (Boston University's MODIS-based land cover product and the GLC2000 data set obtained from the VEGETATION sensor aboard SPOT4) were merged with national-, state-, and county-level crop area and yield statistics at 5 min by 5 min latitude-longitude resolution, which we regrid to match the 2.8˚ x 2.8˚ resolution of MOZART-2.

We use the global chemical transport model (CTM) MOZART-2 (Horowitz et al., 2003, Horowitz, 2006) to simulate O_3 exposure according to precursor emissions specified by the IPCC SRES A2 and B1 scenarios (Nakićenović et al., 2000). MOZART-2 contains a detailed representation of tropospheric ozone-nitrogen oxide-hydrocarbon chemistry, simulating the concentrations and distributions of 63 gas-phase species and 11 aerosol and aerosol precursor species (including sulfate, nitrate, ammonium, black carbon, and organic carbon and mineral dust of 5 size bins with diameters ranging from 0.2 to 20.0 μm). The version of MOZART-2 we use is driven by meteorological inputs every three hours from the National Center for Atmospheric Research (NCAR) Community Climate Model (MACCM3) (Kiehl et al., 1998), has a horizontal resolution of 2.8˚ latitude by 2.8˚ longitude, 34 hybrid sigma-pressure levels up to 4hPa, and 20-minute time step for chemistry and transport.

Emissions for the year 2030 model simulations used in this study (Horowitz, 2006) are based on scaling standard 1990 anthropogenic emissions from Horowitz et al. (2003). Anthropogenic, biogenic, and biomass burning emission inventories for the 1990 simulation are described in detail in Horowitz et al. (2003) and Horowitz (2006). To obtain year 2030 anthropogenic emissions (Table 1), year 1990 anthropogenic emissions (CH_4, N_2O, SO_x, CO, NMVOC, and NO_x) were scaled by the ratio of 2030:1990 total emissions in four geopolitical regions (OECD90, REF, ASIA, and ALM as defined in Table 1) according to the A2 and B1 emissions scenarios. These two scenarios were chosen for analysis because they represent the upper- and lower- boundary projections, respectively, of most O_3 precursor emissions in the year 2030 (the exception being NMVOC emissions, which are highest under the A1B rather than the A2 scenario). These scenarios are also opposite in terms of economic, environmental, and geopolitical driving forces, with the B1 scenario characterized by global cooperation and emphasis on environmental sustainability and the A2 scenario reflecting a more divisive world with greater importance placed on economic growth. Version 1.1 of the SRES marker scenarios A2-ASF and B1-IMAGE were downloaded from http://www.grida.no/climate/ipcc/emission/164.htm. Two-year simulations were performed with the first year used as spin-up and the second year results used for analysis.

In our first paper, we performed a detailed spatial evaluation of simulated year 2000 surface O_3 concentrations with observations according to the two metrics used to calculate O_3 exposure and yield losses (see Section 2.2 for metric definitions). We found that O_3 was fairly well-simulated over Europe and Asia, but that MOZART-2 systematically overestimated surface O_3 concentrations in the central and northeastern U.S. during the summer months, a bias commonly seen in many other global models for reasons that remain unclear (Reidmiller et al., 2009). Because the most significant overestimation of O_3 unfortunately occurs in areas of intensive crop production in the U.S., and because the U.S. is a major producer of all three crops analyzed in this study, we used O_3 concentration measurements over a span of five years (1998-2002) to bias-correct values of simulated O_3 exposure. We perform the same bias-correction here for our year 2030 analysis: we divide simulated O_3 exposure in the U.S. as calculated by the metrics defined in Section 2.2 over each crop growing season by the ratio of modeled:observed O_3 in the same grid cell where measurement data exist from 1998-2002 (where multiple observation sites exist in a single grid cell, we use the average of the measurements to correct simulated values). Where measurements do not exist, we use U.S. eastern and western regional averages of the modeled:observed ratio (dividing line of 90°W), as the model reproduces O_3 in the western U.S. much more accurately than in the East. Like our first paper, O_3 exposure, relative yield loss, crop production loss, and associated cost estimates presented in the following sections for the U.S. are based on these bias-corrected values of O_3 exposure. We recognize that applying the same bias-correction factors based on surface observations from the period 1998-2002 may not be accurate in the year 2030 due to the complicated non-linear chemistry associated with ozone formation. However, we believe this is the best approach given the presence of a systematic bias over the U.S. during the summer months and the inability to use alternative correction factors based on year 2030 surface observations.

2.2. Integrated assessment

Open-top chamber (OTC) field studies that took place primarily in the U.S. and Europe during the 1980s and 1990s established crop-specific concentration:response (CR) functions that predict the yield reduction of a crop at different levels of ozone exposure (Heagle, 1989; Heck, 1989; Krupa et al., 1998). O_3 exposure can be represented in numerous ways, with different statistical indices used to summarize the pattern of ambient O_3 during crop growing seasons. We implement two widely-used metrics, M12 and AOT40, and their CR relationships (Table 2) to calculate crop yield losses globally:

$$\text{M12 (ppbv)} = \frac{1}{n}\sum_{i=1}^{n}[Co_3]_i$$

$$\text{AOT40 (ppmh)} = \sum_{i=1}^{n}([Co_3]_i - 0.04) \quad \text{for } Co_3 \geq 0.04 \text{ ppmv}$$

where:

- $[Co_3]_i$ is the hourly mean O_3 concentration during daylight hours (8:00 – 19:59); and
- n is the number of hours in the 3-month growing season.

We substitute the highly correlated M7 metric (defined like M12 except with daylight hours from 9:00-15:59) when M12 parameter values have not been defined for certain crops. See Avnery et al. (2010) for further detail about these O_3 exposure metrics and their associated uncertainties.

Using hourly surface O_3 simulated by MOZART-2, we calculate O_3 exposure according to the M12 (M7) and AOT40 metrics over the appropriate growing season for soybean, maize, and wheat in each 2.8˚ x 2.8˚ grid cell. "Growing season" is here defined like in VD2009 and Avnery et al. (2010) as the 3 months prior to the start of the harvest period according to crop calendar data from the United States Department of Agriculture (USDA) (USDA, 1984; 2008). We use our distributions of O_3 exposure and the CR functions defined in Table 2 to calculate RYL in every grid cell (RYL_i) for each crop. We then calculate CPL in each grid cell (CPL_i) from RYL_i and the actual crop production in the year 2000 (CP_i) from Ramankutty et al. (2008) and Monfreda et al. (2008) according to:

$$\mathrm{CPL}_i = \frac{\mathrm{RYL}_i}{1-\mathrm{RYL}_i} \times \mathrm{CP}_i \qquad (1)$$

National CPL is determined by summing crop production loss in all the grid cells within each country. We define national RYL (nRYL) as national CPL divided by the theoretical total crop production without O_3 injury (the sum of crop production loss and actual crop production in the year 2000). Because this calculation uses crop data from the year 2000, which likely underestimates production in 2030 due to the projected growing demand for food over the next few decades, our calculations of crop production loss and the cost estimates based upon CPL values (economic loss and potential avoided undernourished individuals, see below) are likely conservative. However, nRYL estimates will be less affected by this issue given the nature of the RYL calculation.

We implement a simple revenue approach to calculate economic loss by multiplying national CPL by producer prices for each crop in the year 2000 as given by the FAO Food Statistics Division (FAOSTAT, http://faostat.fao.org/), which we use as a proxy for domestic market prices due to insufficient information on actual crop prices. This approach has been found to produce estimates of economic loss that are within 20% of those derived using a general equilibrium model with factor feedbacks (Westenbarger and Frisvold, 1995). Finally, we estimate the number of people who could potentially avoid undernourishment if crop losses due to O_3 exposure were eliminated using the FAO definition of the minimum dietary energy requirement (MDER) (kcal/person/day), below which individuals are classified as undernourished. We convert crop production losses to their potential dietary energy equivalents (kcal) using the USDA National Nutrient Database (USDA, 2009), and divide these estimates by national MDER data (the weighted average of the MDERs of different age and sex groups according to each nation's population structure; FAOSTAT, 2008) to determine the number of individuals who could possibly be fed above the FAO undernourishment threshold in the absence of O_3-induced crop losses. Implicit in this calculation is the conservative assumption of zero consumption for would-be undernourished individuals. Because fewer calories are required to avoid undernourishment for those with caloric intake near the MDER threshold (~1600-2000 kcal/person/day) than those with zero consumption, this simplification underestimates the total number of avoided undernourished. Our calculation also assumes that the additional food that could be produced in the absence of O_3 pollution would be used to feed those who are currently undernourished within the country of production, as opposed to being exported, stored, or consumed by those already above the MDER threshold. This simplification likely leads to an overestimate of the possible avoided undernourished in each country. Given these simplifications, our back-of-the-envelope calculations should be interpreted as illustrative, first-order estimates of the contribution of O_3 pollution to global food insecurity. See Avnery et al. (2010) for further details.

3. Results

3.1. Distribution of crop exposure to O_3

Figs. 1 and 2 depict the global distribution of crop exposure to O_3 in 2030 according to the M12 and AOT40 metrics under the A2 and B1 scenarios, respectively. Figures illustrating the change in O_3 exposure from the year 2000 under each scenario are in the Supplementary Material. O_3 is generally higher in the Northern Hemisphere, with exposure during the wheat growing season in Brazil and during the maize growing season in the Democratic Republic of the Congo (DRC) also elevated in both futures (Figs. 1c and 2c). As noted in our companion paper, O_3 exposure during the soybean and maize growing seasons is particularly elevated in the Northern Hemisphere due to the coincidence of these crops' growing seasons with periods of peak summer O_3 concentrations, while the wheat and maize growing seasons in Brazil and the DRC, respectively, coincide with these nations' biomass burning seasons (Avnery et al., 2010). In the A2 scenario, M12 ranges from 30 ppbv to over 80 ppbv for all three crops in the Northern Hemisphere while AOT40 ranges from zero to over 40 ppmh in northern India, eastern China, and parts of the U.S. (Fig. 1).

Northern Hemisphere O_3 exposure is considerably lower in the B1 scenario. M12 ranges from 20-60 ppbv over most continental regions with higher exposures (>70 ppbv) limited to northern India, eastern China, and parts of the southern U.S.; AOT40 is most significantly reduced compared to the A2 scenario in the U.S., Europe, and the Middle East (Fig. 2). However, O_3 exposure still remains largely above the 3 ppmh "critical level" established in Europe for the protection of crops (UN-ECE, 1994; Karenlampi and Skarby, 1996) even under this more optimistic projection of O_3 precursor emissions, particularly during the soybean and maize growing seasons. M12 in the Southern Hemisphere ranges from 10-40 ppbv in both scenarios with the exception of Brazil during the wheat growing season and the DRC during the maize growing season, where O_3 exposure reaches 80 ppbv. AOT40 in the Southern Hemisphere is largely below 5 ppmh with the exception of the two nations listed above, as well as South Africa and parts of northern Australia (Figs. 1-2).

Overall, the highest O_3 exposure in the A2 scenario during the soybean growing season occurs in the U.S., Italy, Turkey, northern India, and China (Fig. 1a). These nations plus the DRC and much of the Mediterranean region also endure the highest levels of O_3 during the maize growing season (Fig. 1b), but O_3 during the wheat growing season is greatest in central Brazil, Bangladesh, India, and the Middle East (Fig. 1c). Under the B1 scenario, the highest levels of O_3 exposure occur primarily in China, India, and to a lesser extent parts of the U.S. during the soybean growing season (Fig. 2a), with these nations plus the DRC and Pakistan experiencing the most elevated O_3 during the maize growing season (Fig. 2b). Wheat-season O_3 exposure in the B1 scenario follows the spatial distribution of the A2 future but with reduced overall magnitude (Fig. 2c).

3.2. Relative yield loss

3.2.1. <u>RYL Year 2030 – A2</u>

The global distribution of national RYL due to O_3 exposure calculated for each crop and metric under the A2 scenario is depicted in Fig. 3. Estimates of soybean and maize (wheat) yield losses are generally larger (smaller) when the M12 rather than the AOT40 metric is used. However, the AOT40 metric and CR functions predict greater yield losses for soybean at higher levels of O_3 exposure than the M12 metric. Under the A2 scenario and using both metrics, O_3-induced RYL of wheat is greatest in Bangladesh (26-80%), Iraq (14-47%), India (12-48%), Jordan (14-44%), and Saudi Arabia (13-43%). The extremely high projected RYL in Bangladesh according to the AOT40 metric is due to a predicted O_3 exposure of over 40 ppmh during the growing season. This value may be overestimated by MOZART-2; however, because no O_3 observations are available from that region we can not evaluate our simulated concentration. For context, Beig et al. (2008) calculated AOT40 from observations in Pune, India between 2003-2006 and reports values near 23 ppmh during the wheat growing season in India (January - March). At this location MOZART-2 predicts a value of 20 ppmh in 2000 over these months. Pune is located in western India, however, where O_3 concentrations tend to be lower than eastern India and Bangladesh during winter (the Bangladeshi wheat growing season).

Although O_3 is elevated during the wheat growing season over much of central Brazil (Fig. 1c), most of this nation's wheat is grown in the south where O_3 exposure is significantly lower. Like the year 2000 scenario, the range of RYL is extremely pronounced for wheat because this crop appears to be resistant to O_3 exposure according to the M12 metric, but extremely sensitive to ozone according to the AOT40 index. This discrepancy may be a consequence of the possibility that wheat is more sensitive to frequent exposure to elevated O_3 (better captured by AOT40) than to long-term exposure to moderate ozone concentrations (better captured by the mean metric) (Wang and Mauzerall, 2004). Soybean RYL under the A2 scenario is estimated to be greatest in China (35-40%), Canada (32-34%), Italy (32-33%), South Korea (31%), and Turkey (27-30%). Yield losses of maize are smaller but still substantial, with the highest losses occurring in the DRC (12-21%), Italy (10-16%), Pakistan (9.1-16%), India (8.9-16%), and Turkey (7.6-14%). Overall, global RYL totals 5.4-26% for wheat, 15-19% for soybean, and 4.4-8.7% for maize.

Table 3 lists the estimated change in regionally and globally aggregated RYL estimates calculated using the M12 and AOT40 metrics under the A2 scenario (year 2030 minus year 2000), as well as their averages. See Table S1 of the Supplementary Material for absolute RYL values by region. We use the same regional aggregations defined in Avnery et al. (2010). On a global scale, O_3-induced RYL is estimated to increase by 1.5-10% for wheat, 0.9-10% for soybean, and 2.1-3.2% for maize. South Asia is projected to suffer the greatest additional wheat RYL (+10% according to the average of metric estimates) followed by Africa and the Middle East (+9.4%), Eastern Europe (+5.8%) and East Asia (+5.0%). Increased soybean yield losses are estimated to be greatest in East Asia (+15%), South Asia (+11%), the EU25 (+7.0%), and Africa and the Middle East (+6.2%). Additional RYL of maize is projected to occur primarily in South and East

Asia (+6.8 and +4.7%, respectively), but with increased losses of ~+3% also estimated for the EU25 and Eastern Europe.

3.2.2. <u>RYL Year 2030 – B1</u>

Fig. 4 depicts the global distribution of national RYL for each crop according to the M12 and AOT40 metrics in the B1 scenario. O_3-induced RYL of wheat is greatest in Bangladesh (15-65%), India (10-37%), Iraq (10-33%), Jordan (10-30%), and Saudi Arabia (10-29%). RYL in Bangladesh is again calculated to be extremely high, as O_3 exposure is projected to be only slightly lower than under the A2 scenario (35-40 ppmh). Soybean RYL in the B1 scenario is projected to be greatest in China (31-32%), South Korea (26-28%), Canada (24-26%), Italy (20-25%), and Pakistan (18-24%). The highest estimated yield loss of maize is expected to occur in the DRC (8.7-16%), India (6.3-12%), Pakistan (6.3-12%), China (5.8-10%), and Italy (5.1-10%). On a global scale, RYL totals 4.0-17% for wheat, 10-15% for soybean, and 2.5-6.0% for maize under the B1 scenario.

Table 4 lists the projected change in regionally and globally aggregated RYL estimates according to the M12 and AOT40 metrics (and their averages); see Table S2 of the Supplementary Material for absolute RYL values by region. Globally, O_3-induced RYL in this more optimistic future is estimated to increase only slightly from 2000 levels: +0.1-1.8% for wheat, +0.7-1.0% for soybean, and +0.3-0.5% for maize. Regional discrepancies are apparent, however, due to differences in projected O_3 precursor emissions among industrialized versus emerging economies. Wheat yield reductions in South Asia are estimated to increase by 4.1% on average, with less severe additional losses (~+1-2%) predicted for other developing regions (Latin America, East Asia, and Africa and the Middle East). North America and the European Union are projected to experience yield gains of wheat as compared to year 2000 (change in RYL of -1.7% and -0.8%, respectively). Additional RYL of soybean is projected to occur primarily in East and South Asia (+8.2 and +4.9%, respectively), with increased losses of ~+2% also estimated for Latin America and Africa and the Middle East. Soybean yield gains of 2-3% are projected for the EU25 and North America. South and East Asia are also expected to suffer additional maize losses under the B1 scenario (+3.5% and +2.2%, respectively); maize RYL in other regions remains largely unchanged from the year 2000.

3.3. *Crop production loss (CPL) and associated economic losses (EL)*

3.3.1. CPL and EL Year 2030 – A2

The combined year 2030 global crop production and economic losses due to O_3 exposure under the A2 scenario are illustrated in Fig. 5. Table 5 lists the change in regionally-aggregated and global CPL for each crop (absolute values are presented in Table S3 of the Supplementary Material), while Figs. 6 and 7 depict the change in CPL and EL, respectively, for the ten countries with the greatest absolute difference (2030A2 – 2000) for each crop individually and combined. We calculate global CPL in the A2 scenario to be 29-178 Mt of wheat (+9-85 Mt from the year 2000), 25-53 Mt of maize (+13-20 Mt), and 28-37 Mt of soybean (+11-13 Mt). South Asia is estimated to suffer the highest additional loss of wheat (19 Mt, average of metric estimates), while East Asia is projected to experience the greatest additional CPL of maize (6.4 Mt) and soybean (4.5 Mt) (Table 5). Total wheat CPL is highest in India (8.5-56 Mt) and China (3.7-33 Mt), followed by the U.S. (2.5-12 Mt). The U.S. is expected to suffer the greatest overall soybean loss (13-18 Mt), followed by China (7.7-10 Mt) and Brazil (1.8-5.7 Mt). CPL of maize is projected to be highest in China (9.7-17 Mt) and the U.S. (8.1-18 Mt), followed by India (1.0-1.9 Mt). On average, global CPL for all three crops totals 175 Mt (119 and 231 Mt from the M12 and AOT40 metrics, respectively); this value represents a 75% increase over our average year 2000 CPL estimate (Avnery et al., 2010). We estimate that global EL due to O_3-induced yield losses totals \$17-35 billion USD_{2000} annually under the A2 scenario, an increase of \$6-17 billion from the year 2000. Most of the economic losses, both in absolute terms and in terms of the greatest change from year 2000 values, occur in China (\$5.6 billion, +\$2.6 billion from the year 2000), India (\$5.2 billion, +\$2.7 billion), and the U.S. (\$4.2 billion, +\$1.1 billion) (Fig. 7). Other countries with notable losses include Iran (over \$1 billion) and Brazil, Turkey, Pakistan, and Syria also each estimated to lose crop value worth \$500 million annually.

3.3.2. CPL and EL Year 2030 – B1

Combined year 2030 global crop production and economic losses in the B1 scenario are illustrated in Fig. 8. Table 6 lists the change in regionally-aggregated and global CPL by crop under this scenario (absolute values are presented in Table S4 of the Supplementary Material), while Figs. 9 and 10 depict the change in CPL and EL, respectively, for the ten countries with the greatest absolute difference (2030B1 – 2000) for each crop individually and combined. Under the 2030B1 scenario, we estimate global CPL to be 21-106 Mt of wheat (+0.8-13 Mt from the year 2000), 14-35 Mt of maize (+1.7-2.9 Mt), and 17-27 Mt of soybean (+1.5-1.9 Mt). We calculate that South Asia will experience the greatest additional wheat CPL in this scenario, but the magnitude is greatly reduced compared to the A2 future (mean estimate of 6.4 Mt as opposed to 19 Mt). The same is true for additional maize and soybean CPL in East Asia, where increases over year 2000 estimates are projected to be 2-3 Mt for each crop (metric averages) (Table 6). Notably, production gains of 5-6 Mt of soybean, maize, and wheat are projected in North America due to reductions in O_3 precursors anticipated under the B1 scenario (Table 1). Thus, relative to 2000, developed countries experience modest yield and crop production gains in the optimistic B1 future, while developing countries suffer higher crop losses due to increased O_3 pollution (although these losses are not as severe as predicted for the A2 scenario).

As in the A2 future, wheat CPL is greatest in India (6.9-35 Mt) and China (3.0-24 Mt), followed by the U.S. (1.6-5.3 Mt). Overall soybean CPL is expected to be highest in the U.S. (7.3-12 Mt), followed by China (6.2-6.5 Mt) and Brazil (0.9-4.6 Mt). Finally, maize CPL is projected to be highest in China (6.9-13 Mt) and the U.S. (3.7-11 Mt), followed by India (0.7-1.4 Mt). Global CPL for all three crops totals 84-137 Mt, approximately 10% greater than our mean year 2000 estimate (Avnery et al., 2010). We estimate global EL in the B1 scenario to total \$12-21 billion USD_{2000} annually, an increase of \$1-3 billion from the year 2000. The majority of the economic losses are expected to occur in China (\$4.1 billion, +\$1.1 billion from the year 2000), India (\$3.4 billion, +\$0.9 billion), and the U.S. (\$2.5 billion, -\$0.6 billion). The U.S., Italy, Japan, and Canada experience monetary gains as compared to the year 2000 due to crop production improvements, although gains in the U.S. are an order of magnitude greater than those of other industrialized nations (Fig. 10). It is important to highlight the fact that despite crop recovery in the U.S. under the B1 scenario, this nation is still among the top three in terms of CPL for each major crop, and is further the third greatest economic loser due to O_3-induced crop losses.

3.4. Implications of O_3-induced crop loss for world hunger

As for our year 2000 scenario, we estimate the number of undernourished persons who could potentially receive adequate caloric intake to meet minimum dietary energy requirements (MDER) if crop losses due to O_3 exposure in the year 2030 were eliminated (the so-called "avoided undernourished") (Fig. 11). Under the A2 scenario, we calculate that a possible 379-890 million people (using the M12 and AOT40 metrics, respectively) could meet the MDER in the absence of O_3-induced agricultural losses, 2-3 times the avoided undernourished in the year 2000. Countries with greatest potential to reduce undernourishment, ranked by the average of metric estimates (where the range represents values calculated by the two metrics), are China (159-273 million individuals), India (66-300 million), Brazil (19-46 million), Pakistan (11-44 million), and Russia (7-43 million). Following the geographic distribution of crop production losses, Africa and the Pacific island nations generally have the smallest potential for avoiding undernourishment by reducing surface O_3 concentrations, while the greatest possible gains exist in Asia, the Middle East, the Former Soviet Union, and parts of South America. This is also true for the B1 scenario, where we calculate a total of 283-545 million people globally could avoid undernourishment, an increase of almost 70% from the mean year 2000 value. Nations with the greatest potential to avoid undernourishment are the same as in the A2 scenario, but with reduced magnitude: China (123-192), India (52-191 million), Brazil (10-38 million), Pakistan (8-30 million), and Russia (4-20 million). While we do not have projections of undernourishment for the year 2030 and therefore cannot calculate the avoided undernourished in terms of the percent of each nation's undernourished population (as we did in our companion paper), we note the most recent estimate (October, 2009) of global hunger in order to contextualize our results: 1.02 billion undernourished people globally, with 642 million in Asia and the Pacific, 265 million in Sub-Saharan Africa, 53 million in Latin American and the Caribbean, and 42 million in the Near East and North Africa (the final 15 million live in developed nations) (FAO, 2009). These numbers illustrate that mitigation of O_3 pollution may be an important strategy in the fight against food insecurity, particularly in Asia, Latin America, and the Middle East where millions of hungry individuals live and where crop losses due to O_3 exposure are projected to rise from already substantial levels. Because increasing agricultural production via pollution mitigation simply requires limiting O_3 precursor emissions rather than bringing additional land under cultivation or adding fertilizer/pesticides to existing fields, the environmental advantages of such an approach extend beyond the direct benefits to crops and human nourishment examined here (see Section 4.3).

4. Discussion

4.1. Comparison with previous work

We compare our results with those of similar studies which calculate RYL, CPL, and EL in the near future. VD2009 use the M12 and AOT40 metrics of O_3 exposure in the year 2030 under the "current legislation scenario" (CLE), which assumes that all currently approved air pollution regulations will be fully implemented and enforced by 2030. Wang and Mauzerall (2004) (hereafter WM2004) use the M7, M12, and two cumulative metrics not implemented here to calculate crop losses in East Asia (China, Japan, and South Korea) in the year 2020 under the IPCC B2 scenario, which lies in between the A2 and B1 storylines in terms of Asian anthropogenic emissions of reactive trace gases (Nakićenović et al., 2000).

VD2009 only report year 2030 crop loss results in terms of the change in RYL, and their optimistic CLE scenario is closest to our B1 simulation. Globally, VD2009 find an increase in RYL for wheat, soybean, and maize of 4%, 0.5%, and 0.2%, respectively, compared to our (B1) mean estimates of 1.0%, 0.8%, and 0.4%. Similar to our results, VD2009 also find that North America and the EU 25 experience stabilization or improvement of yields in 2030, with the greatest additional losses occurring in the Indian subcontinent. WM2004 project much more significant yield reductions in the near future than VD2009 (who report a yield improvement of ~2.5% for Chinese wheat and only marginally increased reductions for the other crops). According to the M7/M12 metric, WM2004 find that year 2020 wheat yield losses in China range from 2-7% depending on the growing season, soybean RYL totals 33%, and maize 16%. Our values match these extremely well (ranges represent the B1 and A2 M7/M12 values, respectively): 3-4% wheat, 31-35% soybean, and 10-13% maize. In South Korea, WM2004 find year 2020 wheat, soybean, and maize RYL to be 8%, 35%, and 4%, respectively, while our RYL estimates are 4% for wheat, 28-31% for soybean, and 8% for maize. Finally, WM2004 estimate Japanese RYL to be 9% for wheat and 28% for soybean (maize is not a major crop in Japan), while our projections are 5-6% for wheat and 23-27% for soybean. Thus despite the differences in datasets, methodologies, model chemistry, and model simulations, our results agree very well with existing estimates of future O_3-induced crop losses but add to the literature by providing a broader range of possible future emissions of ozone precursors and their implications for both agricultural yields and global food security.

4.2. Uncertainties

In our companion paper, we provided a detailed review of the most important sources of uncertainty associated with the integrated assessment approach we use for our analysis (for brevity, only new sources of uncertainty will be highlighted here; see Avnery et al. (2010) for those previously discussed). One of the major sources of uncertainty formerly identified stems from using simulated hourly O_3 concentrations by a global CTM with variable accuracy in reproducing actual O_3 exposure to calculate crop losses. Predicting future O_3 concentrations is even more difficult due to a number of factors: the uncertain trajectory of future emissions of O_3 precursors, the inability to use surface observations to evaluate and bias-correct model simulations, and the potential feedbacks between climate change and O_3 concentrations over the next few decades that are not accounted for by CTMs. We attempt to address the first of these uncertainties by constraining potential future yield losses according to the most optimistic and pessimistic projections of O_3 precursor emissions as specified by the widely-used IPCC SRES scenarios (Nakićenović et al., 2000). Although we cannot perform a model evaluation with surface observations from the year 2030, we use as a proxy bias-correction factors derived from observations in the years 1998-2002 (Avnery et al., 2010), as we expect similar regional biases in our future simulations. Finally, while future predictions of O_3 will be complicated by the potential feedbacks between climate change and ozone, as changes in temperature, precipitation, atmospheric circulation, and other local conditions can affect ozone concentrations that can in turn impact local and regional climate (e.g. Brasseur et al., 2006; Denman et al., 2007; Levy et al., 2008; Wu et al., 2008, Jacob and Winner, 2009; Ming and Ramaswamy, 2009), we expect any changes in O_3 concentrations and distributions due to such feedbacks to be of second order compared to those driven by anthropogenic emissions of ozone precursors.

Climate change may also confound our estimates of future crop yield reductions through altering stomatal conductance: increased temperatures and atmospheric CO_2 concentrations and decreased humidity and soil water content may reduce stomatal openings and therefore the amount of O_3 that enters plant leaves (Mauzerall and Wang, 2001; Fuhrer et al., 2009). In non-irrigated agricultural areas prone to water stress, this affect may be especially significant and may mitigate projected ozone damage. Additionally, climate change may directly impact crop yields through changes in temperature, precipitation patterns, and CO_2 fertilization—however, little is known about the combined effect of climate change and O_3 pollution on agriculture. To investigate this issue, Reilly et al. (2007) use the MIT Integrated Global Systems Model, which includes an updated version of the biogeochemical Terrestrial Ecosystem Model (TEM) that simulates the impact of both climate change and surface ozone on plant productivity. The authors find that while the effects of climate change are generally positive, ozone pollution may more than offset potential climate benefits. For example, yield gains of 50-100% are predicted for much of the world in the year 2100 when only climate impacts are considered, but inclusion of the model's O_3 damage function produces drastic yield reductions: combined climate and O_3 effects reduce yields by 43% in the U.S., 56% in Europe, 45% in India, 64% in China, and 80% in Japan. These results underscore the imperative need for field studies that examine the combined impact on agricultural production of climate change and surface O_3 in order to evaluate model-based studies and accurately predict future crop yields.

Finally, climate change can indirectly affect our estimates of O_3-induced crop yield reductions through its impact on crop growing seasons and crop distributions, which we assume to be the same in our year 2030 analysis as the year 2000. We also do not account for potential adaptation measures farmers may embrace to maximize crop yields in the face of a changing climate or O_3 pollution, such as altering planting/harvesting dates, application of additional fertilizer/water through irrigation, or the development of new cultivars and irrigation infrastructure. Future work will account for potential adaptation through the use of a state-of-the-art agro-economic model, and will also consider feedbacks between crop yields, production areas, and commodity prices to generate a more accurate estimate of the economic cost of agricultural losses.

4.3. Policy Implications

Global agricultural demand is expected to double over the next few decades due to population growth, rising demand for biofuels, and increased meat consumption particularly in developing nations (Tilman et al., 2002; Edgerton, 2009). To meet this future demand, we will need to either bring new terrain under cultivation, or to increase productivity (i.e. yields) on existing agricultural land. The latter option is preferable in order to prevent further ecosystem destruction and the associated loss of biodiversity and increased greenhouse gas emissions. However, improving yields on land currently cultivated through traditional strategies—i.e., increasing agricultural inputs (water, fertilizer, pesticides)—also has detrimental and potentially catastrophic environmental consequences (Tilman et al., 2001). Furthermore, research suggests that in the absence of bioengineering, the historical rate of crop yield improvements experienced since the Green Revolution is declining in many parts of the world, and that the genetic ceiling for maximal yield potential is being approached despite increasing inputs (Peng et al., 1999; Duvick et al., 1999; Tilman et al., 2002). Ozone mitigation provides a means to increase this “ceiling” and the efficiency by which crops use nitrogen, water, and land. Moreover, with mounting evidence that crop yield improvements from CO_2 fertilization may not be as great as previously expected (Long et al., 2005) and that O_3 pollution may more than offset even significant crop yield gains due to climate change (Reilly et al., 2007), this strategy is looking increasingly necessary to adequately feed and fuel a growing population without further environmental degradation. Because tropospheric ozone is a potent greenhouse gas in addition to a noxious air pollutant (Forster et al., 2007), O_3

mitigation would also provide numerous co-benefits to climate and human health (West et al., 2007; Fiore et al., 2008). Ozone abatement measures may further benefit climate indirectly in the absence of an explicit climate change mitigation policy, since many O_3 precursors are emitted by the same sources as CO_2 and other long-lived greenhouse gases.

5. Conclusions

In this study we estimated the global risk to three key staple crops (soybean, maize, and wheat) of surface ozone pollution in the near future (year 2030) using simulated O_3 concentrations under two scenarios of projected O_3 precursor emissions (the IPCC SRES A2 and B1 storylines), two metrics of O_3 exposure (M12 and AOT40), field-based CR relationships, and global maps of agricultural production compiled from satellite data and census yield statistics. We find that for the A2 scenario, global year 2030 relative yield loss of wheat ranges from 5.4-26% (a change of +1.5-10% from year 2000 values), 15-19% for soybean (+0.9-11%), and 4.4-8.7% for maize (+2.1-3.2%), with total crop production loss worth \$17-35 USD_{2000} annually (+\$6-17 billion). In the B1 scenario, we estimate that global relative yield loss totals 4.0-17% for wheat (+0.1-1.8%), 9.5-15% for soybean (+0.7-1.0%), and 2.5-6.0% for maize (+0.3-0.5%), with total losses worth \$12-21 billion annually (+\$1-3 billion). South Asia is projected to suffer the greatest additional loss of wheat, while the largest decrease in soybean and maize yields is expected in East Asia under both future scenarios. Notably, North America is projected to experience production gains of 5-6 Mt of soybean, maize, and wheat under the B1 scenario compared to the year 2000, but estimated to suffer 10-12 Mt of additional crop losses in the A2 scenario. Even with possible gains, however, the U.S. is among the top three losers in terms of CPL and EL in both futures, with China and India comprising the other two nations suffering the highest O_3-induced losses.

We estimate that for the A2 and B1 scenarios, 379-890 million and 283-545 million individuals, respectively, could potentially be lifted above the MDER threshold, more than three-quarters of which would reside in five nations: China, India, Brazil, Pakistan, and Russia. Our CPL, EL, and potential avoided undernourished results should be considered conservative, however, given their derivation from observation-based, year 2000 crop production data that likely underestimate actual agricultural production in the year 2030. Our results suggest that O_3 exposure poses a growing risk to global food security, and that O_3 mitigation may provide the crop yield improvements necessary to feed and fuel a rapidly increasing population without further environmental damage.

Acknowledgements

We thank N. Ramankutty and C. Monfreda for providing us with pre-publication access to their global crop area and yield datasets.

References

Adams, R.M., Glyer, J.D., Johnson, S.L., McCarl, B.A., 1989. A reassessment of the economic effects of ozone on United States agriculture. Journal of the Air Pollution Control Association 39, 960-968.

Avnery, S., Mauzerall, D.L., Liu, J., Horowitz, L.W., 2010. Global crop yield reductions due to surface ozone exposure: 1. Year 2000 crop production losses, economic damage, and implications for world hunger. Submitted to Atmospheric Environment April, 2010.

Beig, G., et al., 2008. Threshold exceedances and cumulative ozone exposure indices at tropical suburban site. Geophysical Research Letters 35, L02802, doi:10.1029/2007GL031434.

Booker, F.L., et al., 2009. The ozone component of global change: Potential effects on agricultural and horticultural plant yield, product quality and interactions with invasive species. Journal of Integrative Plant Biology 51, 337-351.

Brasseur, G.P., et al., 2006. Impact of climate change on the future chemical composition of the global troposphere. Journal of Climate 19, 3932-3951.

Denman, K.L., et al., 2007. Couplings between changes in the climate system and biogeochemistry, in: Solomon, S., et al., (Eds.), Climate Change 2007: The Physical Science Basis. Contribution of Working Group I to the Fourth Assessment Report of the Intergovernmental Panel on Climate Change, Cambridge University Press, Cambridge, United Kingdom and New York, NY, USA.

Dentener, F., et al., 2005. The impact of air pollutant and methane emission controls on tropospheric ozone and radiative forcing: CTM calculations for the period 1990-2030. Atmospheric Chemistry and Physics 5, 1731-1755.

Dentener, F., et al., 2006. The global atmospheric environment for the next generation. Environmental Science and Technology 40, 3586-3594.

Duvick, D.N., Cassman, K.G., 1999. Post-green-revolution trends in yield potential of temperature maize in the north-central United States. Crop Science 39, 1622-1630.

Edgerton, M.D., 2009. Increasing crop productivity to meet global needs for feed, food, and fuel. Plant Physiology 149, 7-13.

FAO, FAOSTAT, Food and Agricultural Organization of the United Nations, accessed May, 2008. Available at http://faostat.fao.org/.

FAO, Food and Agricultural Organization of the United Nations, 2009. The State of Food Insecurity in the World, Rome, Italy.

Fiore, A., et al., 2008. Characterizing the tropospheric ozone response to methane emission controls and the benefits to climate and air quality. Journal of Geophysical Research 113, D08307, doi:10.1029/2007JD009162.

Fiore, A., et al., 2009. Multimodel estimates of intercontinental source-receptor relationships for ozone pollution. Journal of Geophysical Research 114, D04301, doi:10.1029/2008JD010816.

Fiscus, E.L., Booker, F.L., Burkey, K.O., 2005. Crop responses to ozone: uptake, modes of action, carbon assimilation and partitioning. Plant, Cell and Environment 28, 997-1011.

Forster, P., et al., 2007. Changes in atmospheric constituents and radiative forcing, in: Solomon, S., et al., (Eds.), Climate Change 2007: The Physical Science Basis. Contribution of Working Group I to the Fourth Assessment Report of the Intergovernmental Panel on Climate Change, Cambridge University Press, Cambridge, United Kingdom and New York, NY, USA.

Fuhrer, J., 2009. Ozone risk for crops and pastures in present and future climates. Naturwissenschaften 96, 173-194.

Heagle, A.S., 1989. Ozone and crop yield. Annual Review of Phytopathology 27, 397-423.

Heck, W.W., 1989. Assessment of crop losses from air pollutants in the United States, in: MacKenzie, J.J., El-Ashry, M.T. (Eds.), Air Pollution's Toll on Forests and Crops, Yale University Press, New Haven, pp. 235–315.

Horowitz, L.W., et al., 2003. A global simulation of tropospheric ozone and related tracers: description and evaluation of MOZART, Version 2. Journal of Geophysical Research 108, D24, 4784, doi:10.1029/2002JD002853.

Horowitz, L.W. 2006. Past, present, and future concentrations of tropospheric ozone and aerosols: methodology, ozone evaluation, and sensitivity to aerosol wet removal. Journal of Geophysical Research 111, D22211, doi:10.1029/2005JD006937.

Hough, A.D., Derwent, R.G., 1990. Changes in the global concentration of tropospheric ozone due to human activities. Nature 344, 645-650.

Jacob, D., Winner, D., 2009. Effect of climate change on air quality. Atmospheric Environment 43, 51-63.

Karenlampi, L., Skarby, L., 1996. Critical levels for ozone in Europe: testing and finalizing the concepts. Department of Ecology and Environmental Science, University of Kuopio, 363 pp.

Kiehl, J.T., et al., 1999. The National Center for Atmospheric Research Community Climate Model: CCM3. Journal of Climate 11, 1131– 1149.

Krupa, S.V., Nosal, M. Legge, A.H., 1998. A numerical analysis of the combined open-top chamber data from the USA and Europe on ambient ozone and negative crop responses. Environmental Pollution 101, 157-160.

Lesser, V.M., Rawlings, J.O., Spruill, S.E., Somerville, M.C., 1990. Ozone effects on agricultural crops: statistical methodologies and estimated dose-response relationships. Crop Science 30, 148–155.

Levy, H., II, et al., 2008. Strong sensitivity of late 21st century climate to projected changes in short-lived air pollutants, Journal of Geophysical Research 113, D06102, doi:10.1029/2007JD009176.

Long S.P., Ainsworth E.A., Leakey A.D., Morgan P.B., 2005. Global food insecurity: treatment of major food crops with elevated carbon dioxide or ozone under large-scale fully open-air conditions suggests recent models may have overestimated future yields. Philosophical Transactions of the Royal Society B 360, 2011-2020.

Marenco, A., Gouget, H., Nédélec, P., Pagés, J.-P., Karcher, F., 1994. Evidence of a long-term increase in tropospheric ozone from Pic du Midi data series: consequences: positive radiative forcing. Journal of Geophysical Research 99, 16617–16632.

Mauzerall, D. L., Wang, X., 2001. Protecting Agricultural Crops from the Effects of Tropospheric Ozone Exposure: Reconciling Science and Standard Setting in the United States, Europe and Asia. Annual Review of Energy and the Environment 26, 237-268.

Mills, G., et al., 2007. A synthesis of AOT40-based response functions and critical levels of ozone for agricultural and horticultural crops. Atmospheric Environment 41, 2630-2643.

Ming, Y., Ramaswamy, V., 2009. Nonlinear climate and hydrological responses to aerosol effects. Journal of climate 22, doi: 10.1175/2008JCLI2362.1.

Monfreda, C., Ramankutty, N., Foley, J.A., 2008. Farming the planet: 2. Geographic distribution of crop areas, yields, physiological types, and net primary production in the year 2000. Global Biogeochemical Cycles 22, GB1022, doi:10.1029/2007GB002947.

Morgan, P.B., Mies, T.A., Bollero, G.A., Nelson, R.L, Long, S.P., 2006. Season-long elevation of ozone concentration to projected 2050 levels under fully open-air conditions substantially decreases the growth and production of soybean, New Phytologist 170, 333-343.

Nakićenović, N., et al., 2000. Emissions scenarios: a special report of Working Group III of the Intergovernmental Panel on Climate Change, Cambridge Univ. Press, New York, 599 pp.

Oltmans S.J., et al., 2006. Long-term changes in tropospheric ozone. Atmospheric Environment 40, 3156–3173.

Peng, S., et al., 1999. Yield potential of trends of tropical rice since the release of IR8 and the challenge of increasing rice yield potential. Crop Science 39, 1552-1559.

Ramankutty, N., Evan, A., Monfreda, C. Foley, J.A., 2008. Farming the planet: 1. Geographic distribution of global agricultural lands in the year 2000. Global Biogeochemical Cycles 22, GB1003, doi:10.1029/2007GB002952.

Riahi, K., Grübler, A., Nakićenović, N., 2007. Scenarios of long-term socio-economic and environmental development under climate stabilization. Technological Forecasting and Social Change 74, 887-935.

Reidmiller, D.R., et al., 2009. The influence of foreign vs. North American emissions on surface ozone in the U.S., Atmospheric Chemistry and Physics 9, 5027-5042.

Reilly, J., et al., 2007. Global economic effects of changes in crops, pasture, and forests due to changing climate, carbon dioxide, and ozone. Energy Policy 35, 5370-5383.

Tilman, D., et al., 2001. Forecasting agriculturally driven global environmental change. Science 292, 281-284.

Tilman, D., et al., 2001. Agricultural sustainability and intensive production practices. Nature 418, 671-677.

UN-ECE, United Nations Economic Commission for Europe, 1994. Critical levels for ozone - a UN-ECE workshop report. Fuhrer, J., Achermann, B. (Eds.). Swiss Federal Research Station of Agricultural Chemistry and Environmental Health, No. 16. ISSN-1013-154X.

USDA, United States Department of Agriculture, 1994. Major World Crop Areas and Climatic Profiles. In: Agricultural Handbook No. 664. World Agricultural Outlook Board, U.S. Department of Agriculture. Available at: http://www.usda.gov/oce/weather/pubs/Other/MWCACP/MajorWorldCropAreas.pdf.

USDA FAS, United States Department of Agriculture Foreign Agricultural Service. Country Information. Accessed May, 2008. Available at http://www.fas.usda.gov/countryinfo.asp.

USDA, United States Department of Agriculture. National Nutrient Database. Accessed December, 2009. Available at http://www.nal.usda.gov/fnic/foodcomp/search/.

Van Dingenen, R., Raes, F., Krol, M.C., Emberson, L., Cofala, J., 2009. The global impact of O_3 on agricultural crop yields under current and future air quality legislation. Atmospheric Environment 43, 604-618.

Wang X., Mauzerall, D.L., 2004. Characterizing distributions of surface ozone and its impact on grain production in China, Japan and South Korea: 1990 and 2020. Atmospheric Environment 38, 4383–4402.

West, J.J., Fiore, A.M., Naik, V., Horowitz, L.W., Schwarzkopf, M.D., Mauzerall, D.L., 2007. Ozone air quality and radiative forcing consequences of changes in ozone precursor emissions, Geophysical Research Letters 34, L06806, doi:10.1029/2006GL029173.

Westenbarger, D.A., Frisvold, G.B., 1995. Air pollution and farm-level crop yields: an empirical analysis of corn and soybeans. Agricultural and Resource Economics Review 24, 156-165.

Wu, S., et al., 2008. Effects of 2000-2050 global change on ozone air quality in the United States. Journal of Geophysical Research 113, D06302.

Tables

	A2				B1			
	OECD[a]	**REF**[b]	**Asia**[c]	**ALM**[d]	**OECD**[a]	**REF**[b]	**Asia**[c]	**ALM**[d]
CH_4	1.251	1.204	1.631	1.999	0.925	0.931	1.367	1.553
CO	0.973	0.680	1.855	1.522	0.649	0.295	1.192	0.471
NMVOC	1.084	1.590	1.534	1.676	0.685	0.695	1.230	1.060
NO_x	1.326	1.014	2.949	2.832	0.661	0.562	2.163	2.436
SO_x	0.410	0.705	3.198	3.006	0.238	0.406	1.650	3.195

[a] 'OECD' refers to countries of the Organization for Economic Cooperation and Development as of 1990, including the US, Canada, western Europe, Japan and Australia.
[b] 'REF' represents countries undergoing economic reform, including countries of eastern European and the newly independent states of the former Soviet Union.
[c] 'Asia' refers to all developing countries in Asia, excluding the Middle East.
[d] 'ALM' represents all developing countries in Africa, Latin America and the Middle East.

Table 1. Scaling factors used with the 1990 base emissions in MOZART-2 to obtain year 2030 anthropogenic emissions under the A2 and B1 scenarios (Nakićenović et al., 2000).

Crop	Exposure – Relative Yield Relationship	Reference
Soybean	$RY = \exp[-(M12/107)^{1.58}]/\exp[-(20/107)^{1.58}]$	Adams et al. (1989)
	$RY = -0.0116*AOT40 + 1.02$	Mills et al. (2007)
Maize	$RY = \exp[-(M12/124)^{2.83}]/\exp[-(20/124)^{2.83}]$	Lesser et al. (1990)
	$RY = -0.0036*AOT40 +1.02$	Mills et al. (2007)
Wheat	$RY = \exp[-(M7/137)^{2.34}]/\exp[-(25/137)^{2.34}]$ (Winter)	Lesser et al. (1990)
	$RY = \exp[-(M7/186)^{3.2}]/\exp[-(25/186)^{3.2}]$ (Spring)	Adams et al. (1989)
	$RY = -0.0161*AOT40 + 0.99$	Mills et al. (2007)

Table 2. Concentration-response equations used to calculate relative yield losses of soybean, maize, and wheat. RY = relative yield as compared to theoretical yield without O_3-induced losses. See Section 2.2 for definitions of M7, M12 and AOT40. We calculate yield reductions for winter and spring wheat varieties separately and sum them together for our estimates of total O_3-induced wheat yield and crop production losses.

	World	EU 25	FUSSR & E. Europe	N. Am	L. Am.	Africa & M.E.	E. Asia	S. Asia	ASEAN & Australia
Wheat									
AOT40	10.4	4.8	10.0	3.5	6.7	15.3	9.4	17.6	0.3
M7	1.5	1.2	1.5	0.5	1.6	3.4	0.5	3.1	0.0
Mean	**6.0**	**3.0**	**5.8**	**2.0**	**4.1**	**9.4**	**5.0**	**10.4**	**0.1**
Maize									
AOT40	2.1	2.4	2.7	1.4	0.9	1.0	4.1	5.6	2.1
M12	3.2	3.2	3.2	2.1	2.5	2.7	5.3	8.0	3.5
Mean	**2.7**	**2.8**	**3.0**	**1.7**	**1.7**	**1.9**	**4.7**	**6.8**	**2.8**
Soybean									
AOT40	10.5	8.9	0.0	3.8	3.0	5.8	19.7	12.4	1.4
M12	0.9	5.1	0.0	3.0	5.5	6.7	10.7	8.8	5.4
Mean	**5.2**	**7.0**	**0.0**	**3.4**	**4.3**	**6.2**	**15.2**	**10.6**	**3.4**

Table 3. Estimated change in regional relative yield loss (%) (year 2030 – 2000) under the A2 scenario according to the M7, M12 and AOT40 metrics and the metric average.

	World	EU 25	FUSSR & E. Europe	N. Am	L. Am.	Africa & M.E.	E. Asia	S. Asia	ASEAN & Australia
Wheat									
AOT40	1.8	-1.7	-0.1	-2.7	2.3	1.3	3.5	7.1	0.0
M7	0.1	0.2	0.0	-0.6	1.1	0.5	-0.2	1.0	0.0
Mean	**1.0**	**-0.8**	**0.0**	**-1.7**	**1.7**	**0.9**	**1.6**	**4.1**	**0.0**
Maize									
AOT40	0.3	-0.6	-0.1	-0.4	0.1	0.3	2.0	3.0	0.9
M12	0.5	-0.7	-0.1	-0.7	1.2	1.0	2.4	4.0	1.6
Mean	**0.4**	**-0.7**	**-0.1**	**-0.5**	**0.7**	**0.6**	**2.2**	**3.5**	**1.3**
Soybean									
AOT40	1.0	-3.5	0.0	-2.2	1.5	1.0	10.6	5.5	0.1
M12	0.7	-2.1	0.0	-2.3	3.0	3.5	5.7	4.4	1.9
Mean	**0.8**	**-2.8**	**0.0**	**-2.2**	**2.3**	**2.3**	**8.2**	**4.9**	**1.0**

Table 4. Estimated change in regional relative yield loss (%) (year 2030 – 2000) under the B1 scenario according to the M7, M12 and AOT40 metrics and the metric average.

	World	EU 25	FUSSR & E. Europe	N. Am	L. Am.	Africa & M.E.	E. Asia	S. Asia	ASEAN & Australia
Wheat									
AOT40	84.6	6.2	11.3	4.0	1.3	12.3	14.5	34.9	0.1
M7	8.6	1.2	1.3	0.5	0.3	1.7	0.5	3.1	0.0
Mean	**46.6**	**3.7**	**6.3**	**2.2**	**0.8**	**7.0**	**7.5**	**19.0**	**0.0**
Maize									
AOT40	12.6	1.0	0.8	3.8	0.6	0.3	5.2	0.8	0.2
M12	20.4	1.5	1.0	6.1	1.8	0.8	7.6	1.3	0.3
Mean	**16.5**	**1.3**	**0.9**	**4.9**	**1.2**	**0.5**	**6.4**	**1.0**	**0.3**
Soybean									
AOT40	12.8	0.1	0.0	3.9	1.9	0.0	5.9	0.9	0.0
M12	11.4	0.1	0.0	3.5	4.0	0.1	3.1	0.7	0.0
Mean	**12.1**	**0.1**	**0.0**	**3.7**	**3.0**	**0.0**	**4.5**	**0.8**	**0.0**

Table 5. Estimated change in regional crop production loss (million metric tons) (year 2030 – 2000) under the A2 scenario according to the M7, M12, and AOT40 metrics and the metric average.

	World	EU 25	FUSSR & E. Europe	N. Am	L. Am.	Africa & M.E.	E. Asia	S. Asia	ASEAN & Australia
Wheat									
AOT40	13.0	-2.0	-0.1	-2.8	0.4	0.8	4.9	11.8	0.0
M7	0.8	0.2	0.0	-0.5	0.2	0.2	-0.2	1.0	0.0
Mean	**6.9**	**-0.9**	**0.0**	**-1.7**	**0.3**	**0.5**	**2.3**	**6.4**	**0.0**
Maize									
AOT40	1.7	-0.3	0.0	-1.1	0.1	0.1	2.4	0.4	0.1
M12	2.9	-0.3	0.0	-1.9	0.9	0.3	3.2	0.6	0.1
Mean	**2.3**	**-0.3**	**0.0**	**-1.5**	**0.5**	**0.2**	**2.8**	**0.5**	**0.1**
Soybean									
AOT40	1.9	0.0	0.0	-2.1	0.9	0.0	2.8	0.4	0.0
M12	1.5	0.0	0.0	-2.5	2.2	0.0	1.5	0.3	0.0
Mean	**1.7**	**0.0**	**0.0**	**-2.3**	**1.5**	**0.0**	**2.1**	**0.3**	**0.0**

Table 6. Estimated change in regional crop production loss (million metric tons) (year 2030 – 2000) under the B1 scenario according to the M7, M12, and AOT40 metrics and the metric average.

Figure Captions

Fig. 1. Global distribution of O_3 exposure according to the M12 (left panels) and AOT40 (right panels) metrics under the 2030 A2 scenario during the respective growing seasons in each country (where crop calendar data are available) of (a) soybean, (b) maize, and (c) wheat. Minor producing nations not included in this analysis (where growing season data were unavailable) together account for <5% of global production of each crop. Values in the U.S. have been corrected using observation data as described in Section 2.1.

Fig. 2. Global distribution of O_3 exposure according to the M12 (left panels) and AOT40 (right panels) metrics under the 2030 B1 scenario during the respective growing seasons in each country (where crop calendar data are available) of (a) soybean, (b) maize, and (c) wheat. Minor producing nations not included in this analysis (where growing season data were unavailable) together account for <5% of global production of each crop. Values in the U.S. have been corrected using observation data as described in Section 2.1.

Fig. 3. National relative yield loss under the 2030 A2 scenario according to the M12 (left panels) and AOT40 (right panels) metrics for (a) soybean, (b) maize, and (c) wheat.

Fig. 4. National relative yield loss under the 2030 B1 scenario according to the M12 (left panels) and AOT40 (right panels) metrics for (a) soybean, (b) maize, and (c) wheat.

Fig. 5. Total crop production loss (CPL, left panels) and economic loss (EL, right panels) under the 2030 A2 scenario for all three crops derived from (a) M12 and (b) AOT40 estimates of O_3 exposure.

Fig. 6. Change in crop production loss (CPL, million metric tons) for the ten countries with highest absolute difference in estimated mean CPL between 2000 and 2030 under the A2 scenario using the M12 and AOT40 metrics for a) soybean, b) maize, c) wheat, and d) total CPL.

Fig. 7. Change in economic loss (EL, million USD_{2000}) for the ten countries with highest absolute difference in estimated mean EL between 2000 and 2030 under the A2 scenario using the M12 and AOT40 metrics for a) soybean, b) maize, c) wheat, and d) total EL.

Fig. 8. Total crop production loss (CPL, left panels) and economic loss (EL, right panels) under the 2030 B1 scenario for all three crops derived from (a) M12 and (b) AOT40 estimates of O_3 exposure.

Fig. 9. Change in crop production loss (CPL, million metric tons) for the ten countries with highest absolute difference in estimated mean CPL between 2000 and 2030 under the B1 scenario using the M12 and AOT40 metrics for a) soybean, b) maize, c) wheat, and d) total CPL.

Fig. 10. Change in economic loss (EL, million USD_{2000}) for the ten countries with highest absolute difference in estimated mean EL between 2000 and 2030 under the B1 scenario using the M12 and AOT40 metrics for a) soybean, b) maize, c) wheat, and d) total EL.

Fig. 11. Potential number of undernourished individuals avoided if crop losses from O_3 exposure could be eliminated derived from (a) M12 and (b) AOT40 estimates of year 2030 crop production losses (CPL) under the A2 (left panels) and B1 (right panels) scenarios. Dark shaded nations represent countries for which CPL was calculated but where FAO data on undernourishment do not exist.

Supplementary Material

	World	EU 25	FUSSR & E. Europe	N. Am	L. Am.	Africa & M.E.	E. Asia	S. Asia	ASEAN & Australia
Wheat									
AOT40	25.8	16.9	21.5	14.5	12.6	35.5	25.7	44.4	1.3
M7	5.4	4.5	4.0	3.1	3.0	9.4	3.8	11.2	0
Mean	**15.6**	**10.7**	**12.7**	**8.8**	**7.8**	**22.4**	**14.7**	**27.8**	**0.6**
Maize									
AOT40	4.4	5.9	5.1	3.4	1	1.6	7.9	8.9	2.3
M12	8.7	11.0	9.7	7.2	4.6	5.2	13.3	16.0	5.9
Mean	**6.5**	**8.5**	**7.4**	**5.3**	**2.9**	**3.4**	**10.6**	**12.5**	**4.1**
Soybean									
AOT40	19.0	32.8	-	15.7	3.2	7.8	40.6	15.6	1
M12	14.8	32.4	-	19.9	11.9	16.6	35.4	22.0	9.1
Mean	**16.4**	**32.6**	**-**	**17.8**	**7.5**	**12.2**	**38.0**	**18.8**	**5.3**

Table S1. Estimated year 2030 regional relative yield loss (%) due to O_3 exposure under the A2 scenario according to the M7, M12 and AOT40 metrics and the metric average.

	World	EU 25	FUSSR & E. Europe	N. Am	L. Am.	Africa & M.E.	E. Asia	S. Asia	ASEAN & Australia
Wheat									
AOT40	17.2	10.4	11.4	8.2	8.1	21.4	19.7	33.8	1.0
M7	4.0	3.4	2.4	2.0	2.6	6.4	3.1	9.2	0
Mean	**10.6**	**6.9**	**6.9**	**5.1**	**5.4**	**13.9**	**11.4**	**21.5**	**0.5**
Maize									
AOT40	2.5	2.9	2.2	1.6	0	0.8	5.8	6.3	1.2
M12	6.0	7.2	6.4	4.4	3.3	3.6	10.3	12.0	4.0
Mean	**4.3**	**5.0**	**4.3**	**3.0**	**1.9**	**2.2**	**8.0**	**9.1**	**2.6**
Soybean									
AOT40	9.5	20.4	-	9.8	1.7	3.0	31.5	8.6	0
M12	14.6	25.3	-	14.6	9.4	13.3	30.5	17.6	5.7
Mean	**12.1**	**22.9**	**-**	**12.2**	**5.5**	**8.2**	**31.0**	**13.1**	**2.9**

Table S2. Estimated year 2030 regional relative yield loss (%) due to O_3 exposure under the B1 scenario according to the M7, M12 and AOT40 metrics and the metric average.

	World	EU 25	FUSSR & E. Europe	N. Am	L. Am.	Africa & M.E.	E. Asia	S. Asia	ASEAN & Australia
Wheat									
AOT40	178.0	19.2	21.5	14.5	2.3	22.8	33.2	64.4	0.3
M7	29.3	4.4	3.2	2.7	0.5	4.3	3.8	10.2	0
Mean	**103.7**	**11.8**	**12.4**	**8.6**	**1.4**	**13.5**	**18.5**	**37.3**	**0.1**
Maize									
AOT40	25.2	2.4	1.4	9.0	0.9	0.5	9.7	1.2	0
M12	52.5	4.8	2.8	19.9	3.3	1.5	17.4	2.3	0.5
Mean	**38.9**	**3.6**	**2.1**	**14.5**	**2.1**	**1.0**	**13.5**	**1.8**	**0.4**
Soybean									
AOT40	27.6	0.3	-	14.4	2.0	0	9.7	1.0	0
M12	37.2	0.3	-	19.2	8.1	0	7.8	1.6	0
Mean	**32.4**	**0.3**	**-**	**16.8**	**5.0**	**0**	**8.8**	**1.3**	**0**

Table S3. Estimated year 2030 regional crop production loss (million metric tons) due to O_3 exposure under the A2 scenario according to the M7, M12 and AOT40 metrics and the metric average.

	World	EU 25	FUSSR & E. Europe	N. Am	L. Am.	Africa & M.E.	E. Asia	S. Asia	ASEAN & Australia
Wheat									
AOT40	106.4	10.9	10.1	7.7	1.4	11.3	23.6	41.3	0.2
M7	21.5	3.3	2.0	1.7	0.4	2.9	3.0	8.2	0
Mean	**64.0**	**7.1**	**6.0**	**4.7**	**0.9**	**7.1**	**13.3**	**24.7**	**0.1**
Maize									
AOT40	14.4	1.1	0.6	4.2	0.3	0.2	6.9	0.8	0
M12	35.0	3.0	1.8	11.9	2.3	1.0	13.0	1.7	0.4
Mean	**24.7**	**2.1**	**1.2**	**8.0**	**1.3**	**0.6**	**10.0**	**1.2**	**0.2**
Soybean									
AOT40	16.7	0.2	-	8.4	1.0	0	6.6	0.5	0
M12	27.2	0.2	-	13.2	6.2	0	6.2	1.2	0
Mean	**22.0**	**0.2**	**-**	**10.8**	**3.6**	**0**	**6.4**	**0.9**	**0**

Table S4. Estimated year 2030 regional crop production loss (million metric tons) due to O_3 exposure under the B1 scenario according to the M7, M12 and AOT40 metrics and the metric average.

SM. 1. Global distribution of the change in O_3 exposure under the 2030A2 scenario according to the M12 (left panels) and AOT40 (right panels) metrics during the respective growing seasons in each country (where crop calendar data are available) of (a) soybean, (b) maize, and (c) wheat. Minor producing nations not included in this analysis (where growing season data were unavailable) together account for <5% of global production of each crop. Values in the U.S. have been corrected using observation data as described in Section 2.1.

SM. 2. Global distribution of the change in O_3 exposure under the 2030B1 scenario according to the M12 (left panels) and AOT40 (right panels) metrics during the respective growing seasons in each country (where crop calendar data are available) of (a) soybean, (b) maize, and (c) wheat. Minor producing nations not included in this analysis (where growing season data were unavailable) together account for <5% of global production of each crop. Values in the U.S. have been corrected using observation data as described in Section 2.1.

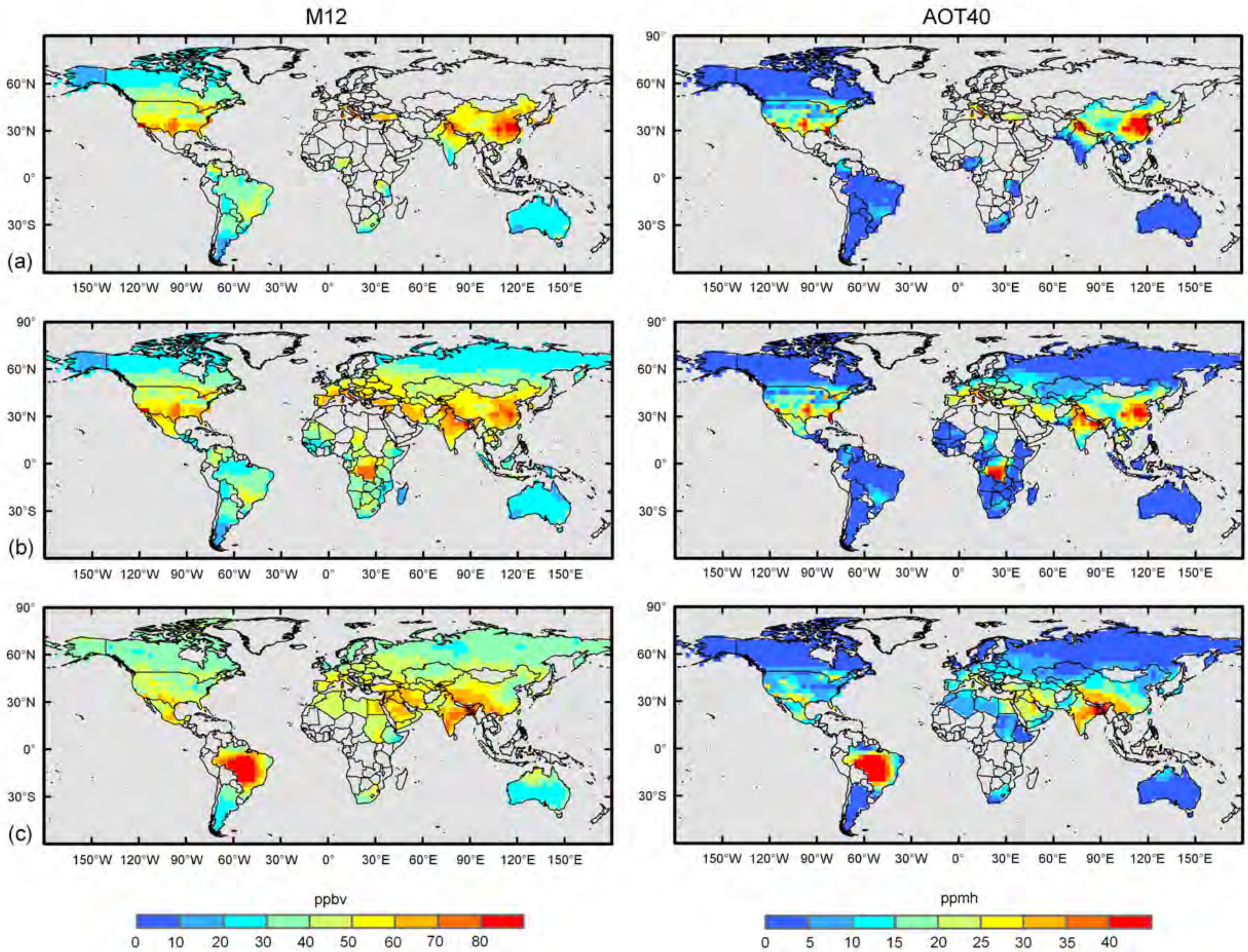

Fig. 1. Global distribution of O_3 exposure according to the M12 (left panels) and AOT40 (right panels) metrics under the 2030 A2 scenario during the respective growing seasons in each country (where crop calendar data are available) of (a) soybean, (b) maize, and (c) wheat. Values in the U.S. have been corrected using observation data as described in Section 2.1.

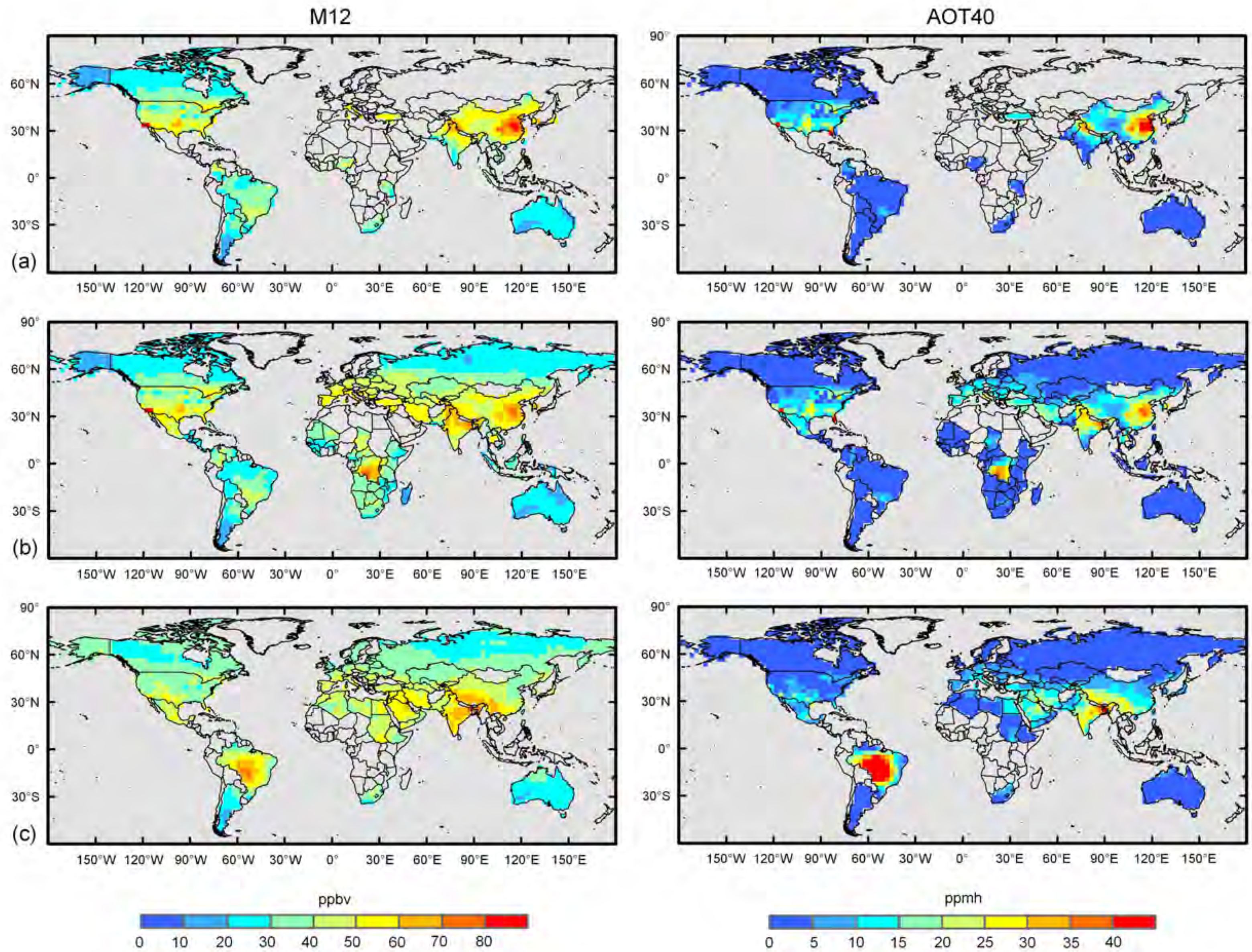

Fig. 2. Global distribution of O_3 exposure according to the M12 (left panels) and AOT40 (right panels) metrics under the 2030 B1 scenario during the respective growing seasons in each country (where crop calendar data are available) of (a) soybean, (b) maize, and (c) wheat. Values in the U.S. have been corrected using observation data as described in Section 2.1.

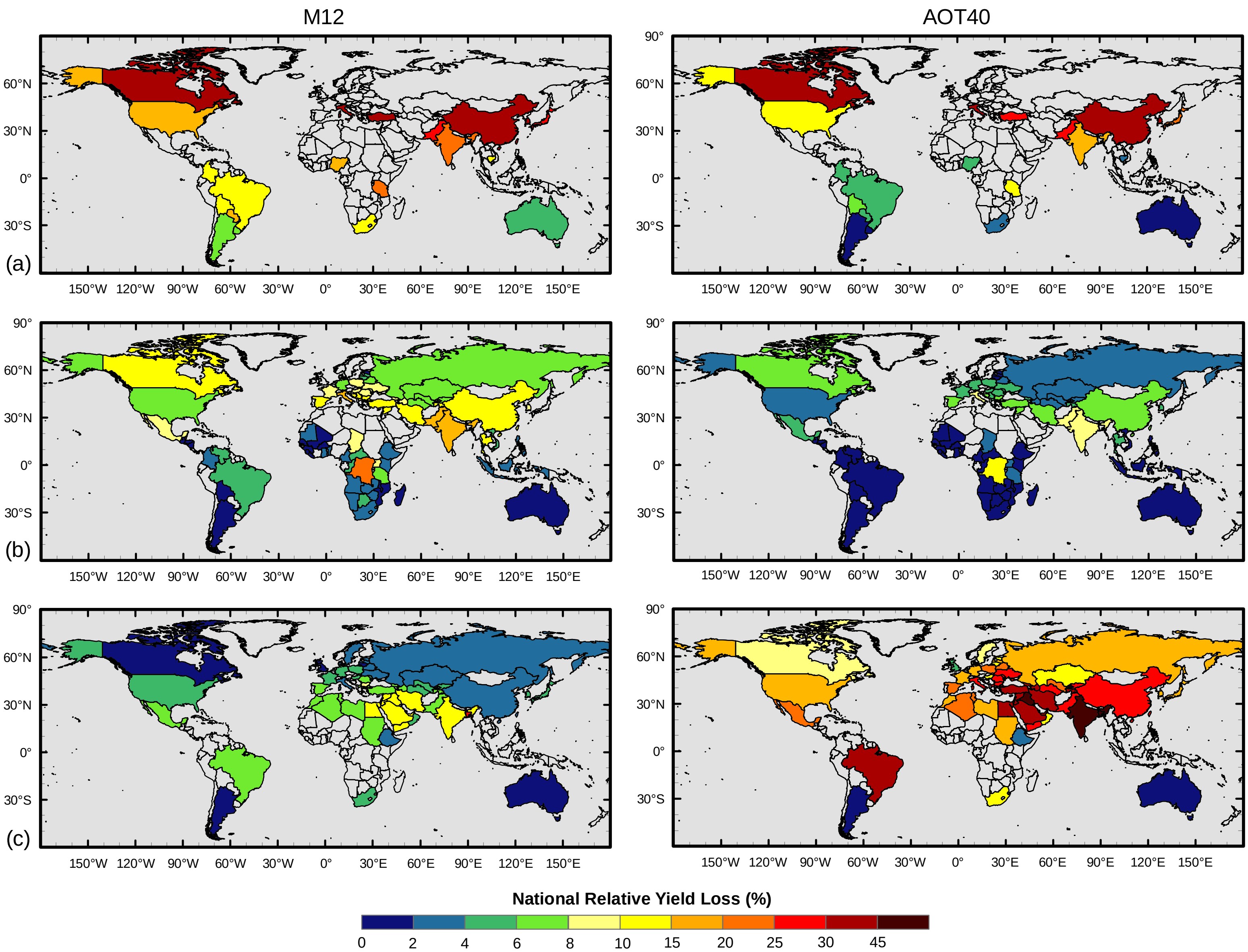

Fig. 3. National relative yield loss under the 2030 A2 scenario according to the M12 (left panels) and AOT40 (right panels) metrics for (a) soybean, (b) maize, and (c) wheat.

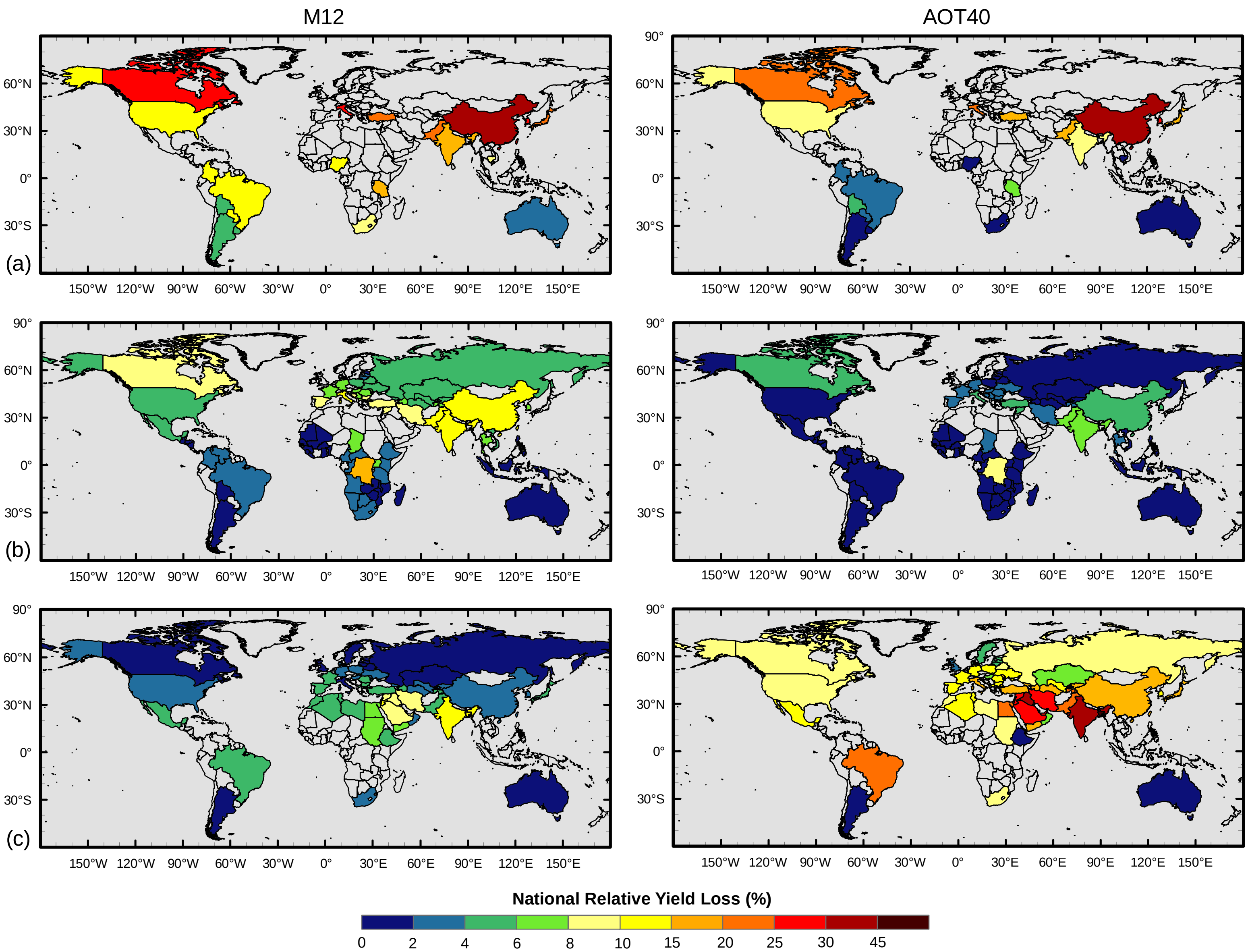

Fig. 4. National relative yield loss under the 2030 B1 scenario according to the M12 (left panels) and AOT40 (right panels) metrics for (a) soybean, (b) maize, and (c) wheat.

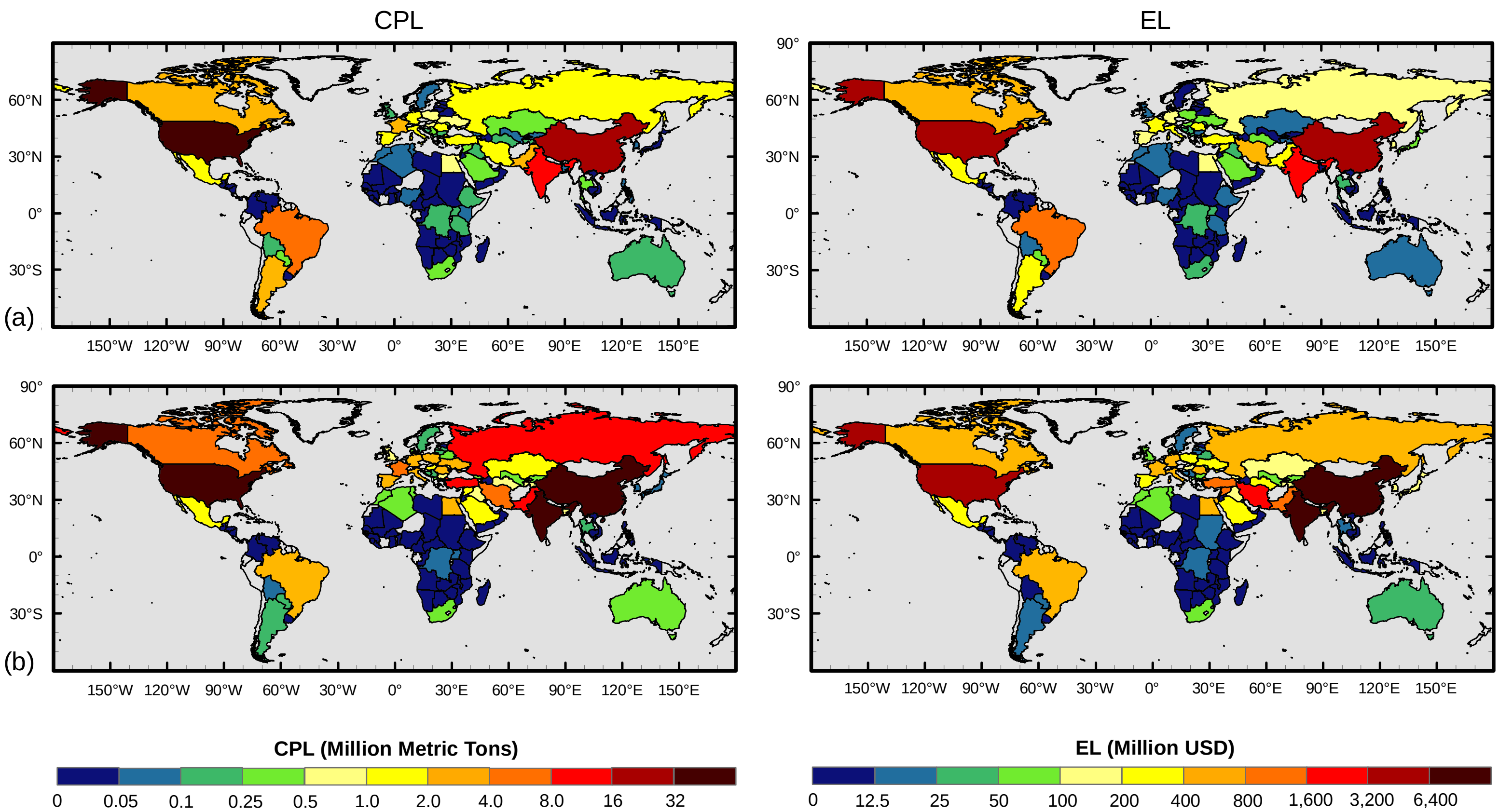

Fig. 5. Total crop production loss (CPL, left panels) and economic loss (EL, right panels) under the 2030 A2 scenario for all three crops derived from (a) M12 and (b) AOT40 estimates of O_3 exposure.

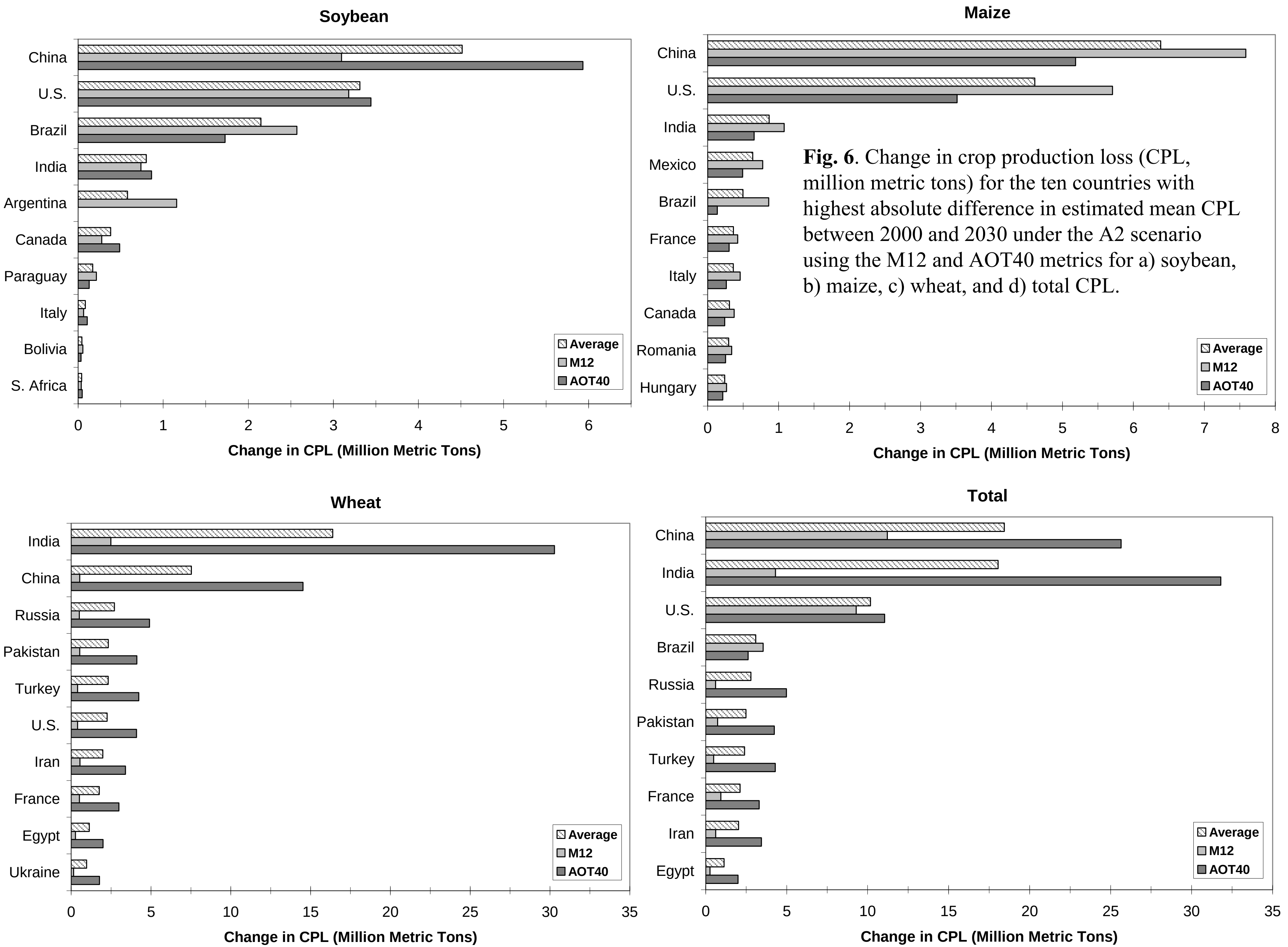

Fig. 6. Change in crop production loss (CPL, million metric tons) for the ten countries with highest absolute difference in estimated mean CPL between 2000 and 2030 under the A2 scenario using the M12 and AOT40 metrics for a) soybean, b) maize, c) wheat, and d) total CPL.

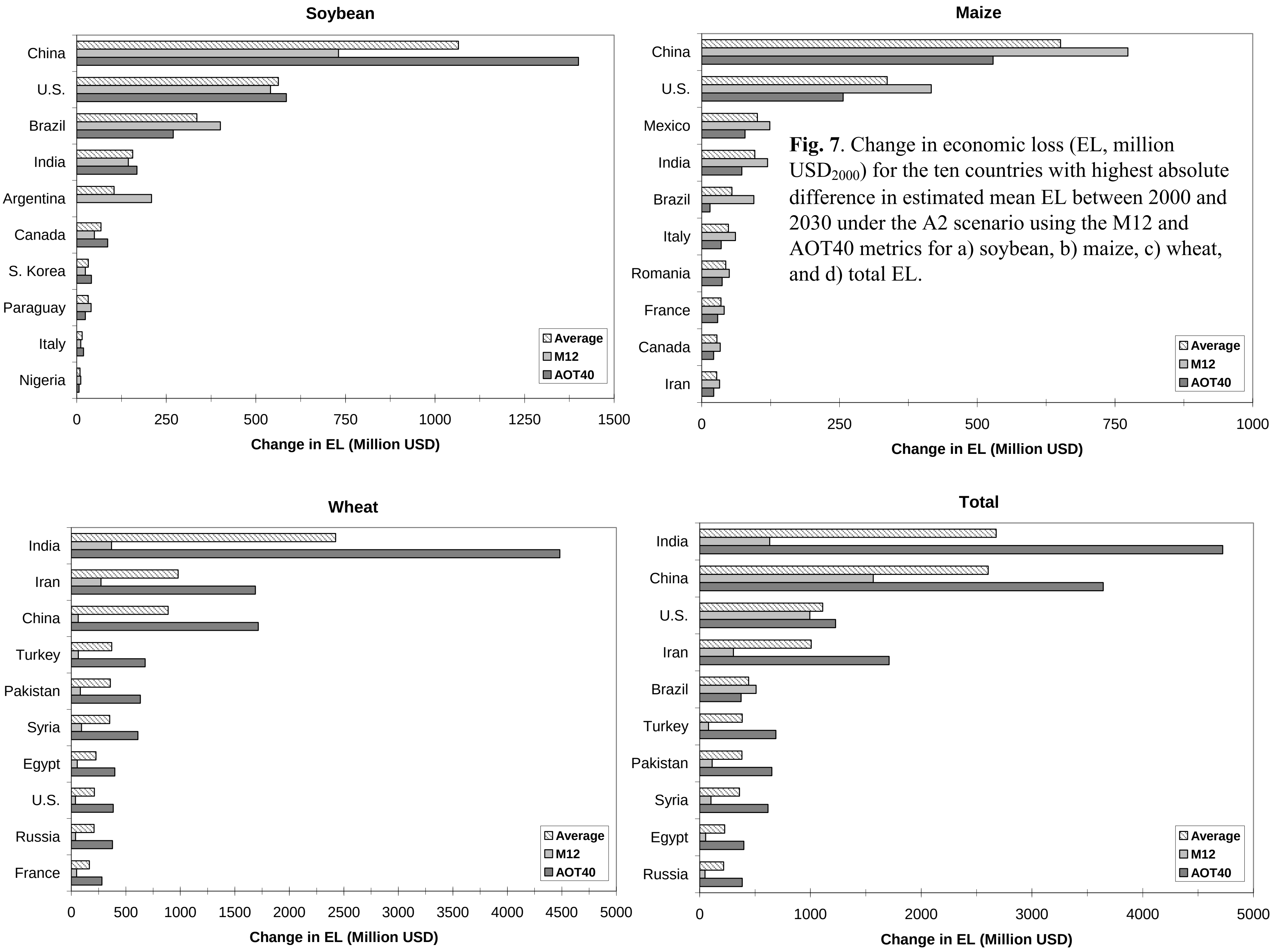

Fig. 7. Change in economic loss (EL, million USD_{2000}) for the ten countries with highest absolute difference in estimated mean EL between 2000 and 2030 under the A2 scenario using the M12 and AOT40 metrics for a) soybean, b) maize, c) wheat, and d) total EL.

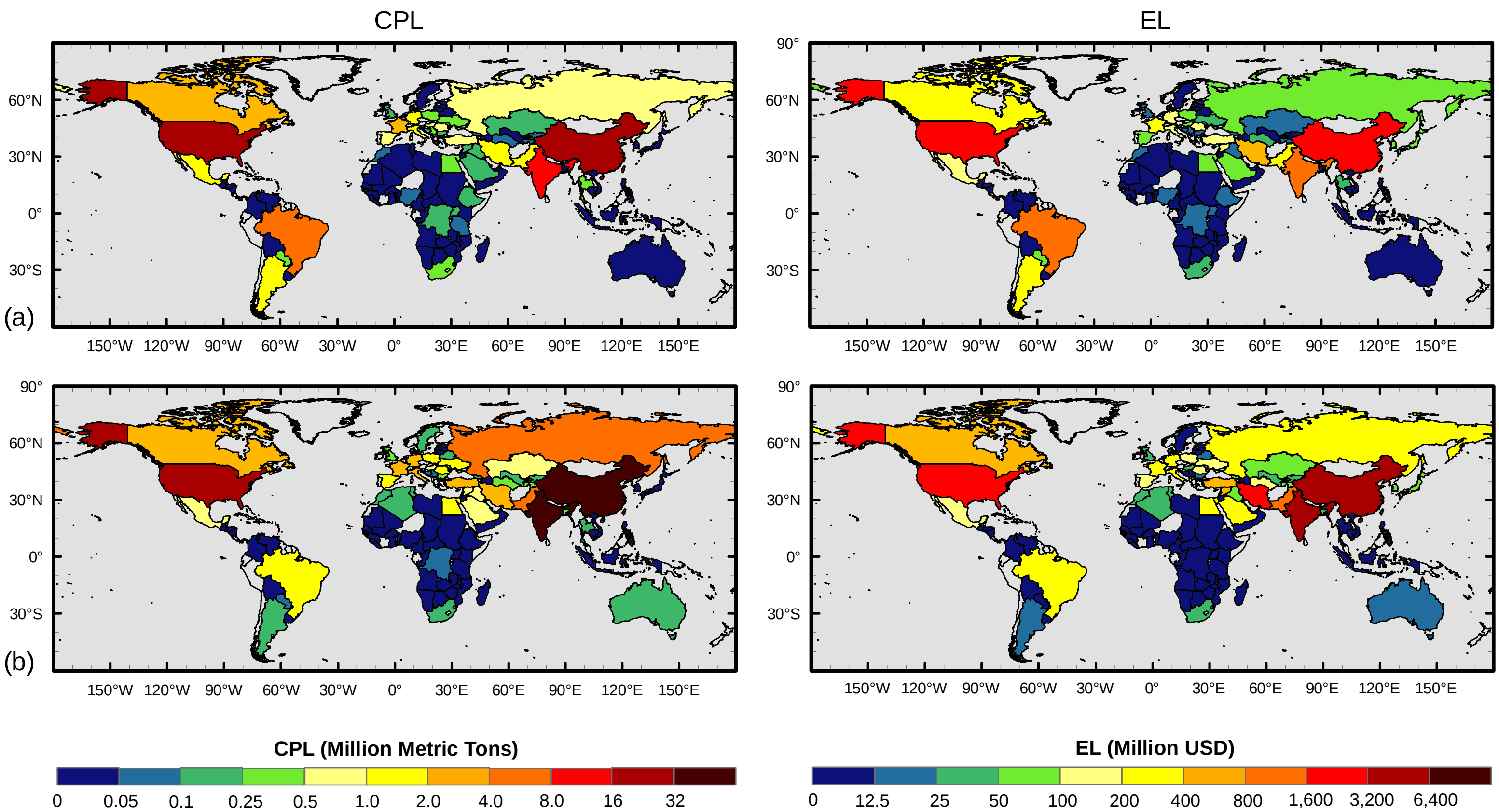

Fig. 8. Total crop production loss (CPL, left panels) and economic loss (EL, right panels) under the 2030 B1 scenario for all three crops derived from (a) M12 and (b) AOT40 estimates of O_3 exposure.

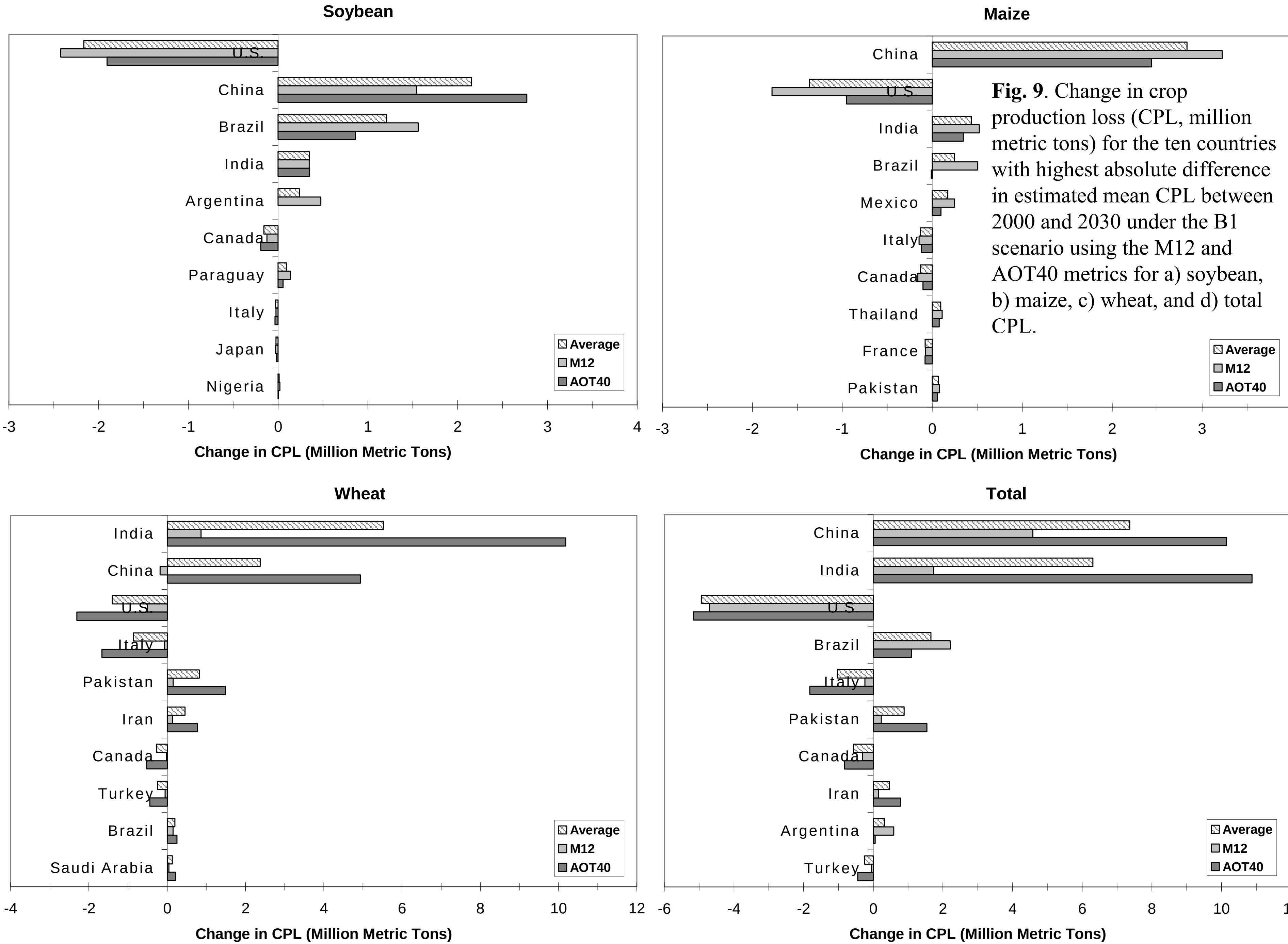

Fig. 9. Change in crop production loss (CPL, million metric tons) for the ten countries with highest absolute difference in estimated mean CPL between 2000 and 2030 under the B1 scenario using the M12 and AOT40 metrics for a) soybean, b) maize, c) wheat, and d) total CPL.

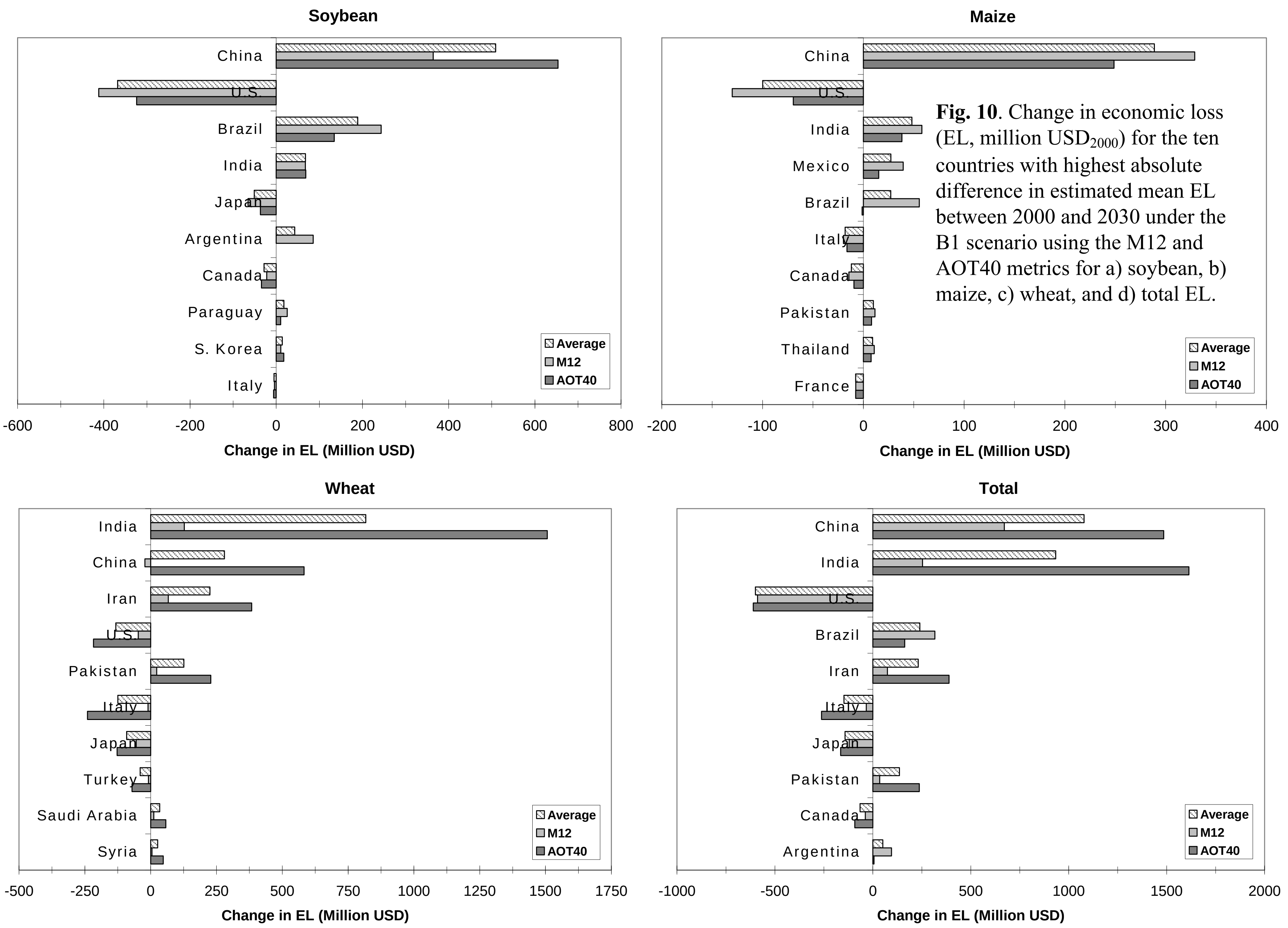

Fig. 10. Change in economic loss (EL, million USD_{2000}) for the ten countries with highest absolute difference in estimated mean EL between 2000 and 2030 under the B1 scenario using the M12 and AOT40 metrics for a) soybean, b) maize, c) wheat, and d) total EL.

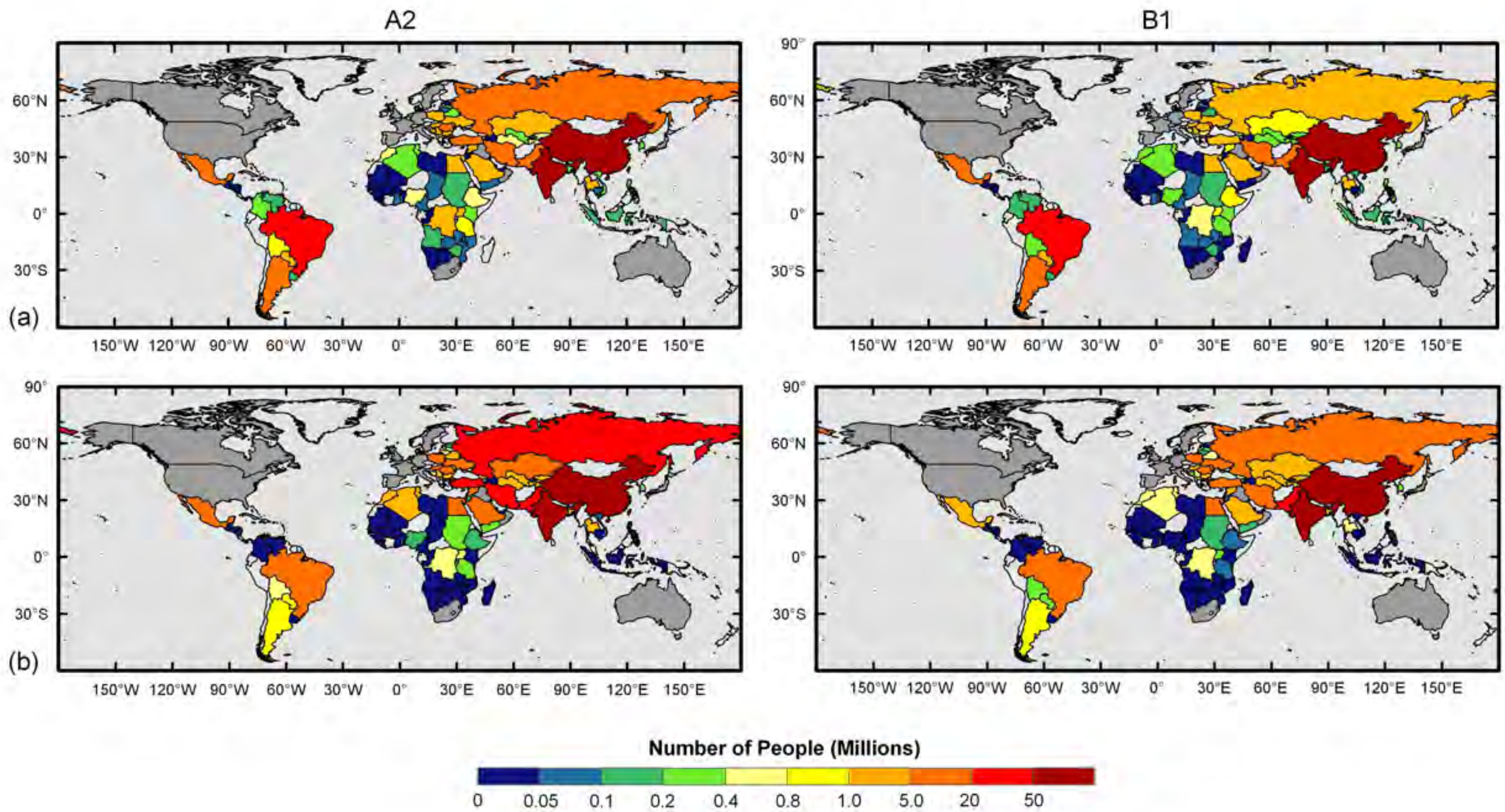

Fig. 11. Potential number of undernourished individuals avoided if crop losses from O_3 exposure could be eliminated derived from (a) M12 and (b) AOT40 estimates of year 2030 crop production losses (CPL) under the A2 (left panels) and B1 (right panels) scenarios. Dark shaded nations represent countries for which CPL was calculated but where FAO data on undernourishment do not exist.